Simulation analysis of an ABS control system for electric vehicles equipped with an electro-mechanical brake

Ritoša, Matija

UNIVERSITY OF ZAGREB
FACULTY OF MECHANICAL ENGINEERING AND NAVAL ARCHITECTURE

MASTER'S THESIS

Matija Ritoša

Zagreb, 2020.

UNIVERSITY OF ZAGREB
FACULTY OF MECHANICAL ENGINEERING AND NAVAL ARCHITECTURE

MASTER'S THESIS

Mentor:

prof. dr. sc. Joško Deur

Student:

Matija Ritoša

Zagreb, 2020.

IZJAVA

Izjavljujem da sam ovaj rad izradio samostalno koristeći znanja stečena tijekom studija i navedenu literaturu.

STATEMENT

I declare that I have done this study using knowledge and skills gained during my university studies and using specified scientific literature.

ZAHVALA

Ovim putem htio bih se zahvaliti svome mentoru prof. dr. sc. Jošku Deuru na prihvaćanju mentorstva. Također se zahvaljujem za sve savjete i podršku prilikom izrade rada.

Nadalje, zahvaljujem se mr. sc. Nikoli Naranči zbog pružene mogućnosti izrade rada unutar tvrtke AVL-AST d.o.o. te svim kolegama na korisnim savjetima prilikom izrade rada. Zahvaljujem se i Mariu Teitzeru iz tvrtke AVL List GmbH koji je s konstantom podrškom i posvećenosti pridonio u izradi ovoga rada.

Posebne zahvale mojim roditeljima, Andreji i Mirijanu te sestri Luciji, koji su uz mene čitav život i studiranje, te vam hvala za svu pomoć u teškim trenutcima.

Naposlijetku, hvala svim mojim prijateljima koji su učinili studiranje jednim od najljepših perioda mog života.

ACKNOWLEDGMENTS

I would like to thank my mentor Professor Joško Deur for accepting the mentorship for this thesis, as well as for all suggestions and support during writing of this thesis.

Also, I would like to thank MPhil Nikola Naranča for giving me the opportunity to make my thesis within AVL-AST d.o.o. and thanks to all of my colleagues on useful suggestions. I would like to thank Mario Teitzer on constant support and dedication which contributed this thesis.

Special thanks, to my parents, Andreja and Mirijan, and to my sister Lucija, who have been beside me during my whole life and studying and thank you for all the help in tough times.

Finally, thanks to all my friends who made studying one of the best periods of my life.

SVEUČILIŠTE U ZAGREBU
FAKULTET STROJARSTVA I BRODOGRADNJE
Središnje povjerenstvo za završne i diplomske ispite
Povjerenstvo za diplomske ispite studija strojarstva za smjerove:
procesno-energetski, konstrukcijski, brodostrojarski i inženjersko modeliranje i računalne simulacije

Sveučilište u Zagrebu Fakultet strojarstva i brodogradnje	
Datum:	Prilog:
Klasa: 602 - 04 / 20 - 6 / 3	
Ur. broj: 15 - 1703 - 20 -	

DIPLOMSKI ZADATAK

Student: **Matija Ritoša** Mat. br.: 0035202036

Naslov rada na hrvatskom jeziku: **Simulacijska analiza sustava ABS upravljanja za električna vozila opremljena elektromehaničkom kočnicom**

Naslov rada na engleskom jeziku: **Simulation analysis of an ABS control system for electric vehicles equipped with an electro-mechanical brake**

Opis zadatka:

Future electric vehicles are expected to be equipped with electro-mechanical brakes (EMB) for improved performance of anti-lock braking systems (ABS) when compared to the use of conventional, hydraulic brake systems. The EMB can provide fast and continuous actuation as a prerequisite for ultimate longitudinal tire slip control aimed at shortening the braking distance. The goal of this thesis is to proof feasibility and analyse the performance of an EBS- and electric traction motor-based ABS controller within a simulation environment. The simulation study should account for relevant measurement signal delays, actuator dynamics of EMB and e-motors, and parameter variations and uncertainties of the vehicle (load conditions, tyre) and road surface. To this end, the main tasks of the thesis are as follows:

1. Building-up a simulation environment based on AVL VSM™ vehicle dynamics simulation software and integration of available ABS controllers within MATLAB/Simulink for co-simulation with AVL VSM™;
2. Updating the vehicle dynamics simulation model with an EMB and electric traction motors as ABS actuators;
3. Proofing feasibility of the built-up ABS controller by conducting typical brake manoeuvres on different road surfaces with continuous and varying coefficient of friction (e.g. μ-split and μ-step) and estimate a potential of the developed approach by means of simulation;
4. Assessing relevant key performance indicators (KPIs), such as ABS controller robustness against parameter and signal uncertainties, braking distance and vehicle dynamics stability compared to the conventional brake system;
5. Validating the ABS controller in demonstrator vehicle.

The literature used should be revealed through the list of references and any eventually received assistance/support should be acknowledged.

Zadatak zadan:	Datum predaje rada:	Predviđeni datum obrane:
5. ožujka 2020.	7. svibnja 2020.	11. – 15.5.2020.

Zadatak zadao:

Prof. dr. sc. Joško Deur

Predsjednica Povjerenstva:

Prof. dr. sc. Tanja Jurčević Lulić

CONTENT

CONTENT I
LIST OF FIGURES III
LIST OF TABLES V
LIST OF SYMBOLS VI
LIST OF ABBREVIATIONS VIII
SAŽETAK IX
SUMMARY X
PROŠIRENI SAŽETAK i
1. INTRODUCTION 1
1.1. Motivation 1
2. ELECTROMECHANICAL BRAKE MODEL 5
2.1. Basic working principle and characteristics of electromechanical brakes 5
2.2. Theoretical and experimental mathematical models 8
2.3. System identification of EMB dynamics 9
3. WHEEL SLIP CONTROL 13
3.1. Tire modeling 13
3.2. Problem description 15
3.3. Slip dynamics 17
3.4. Gain-Scheduling PI control 18
3.4.1. Gain Scheduling 19
3.4.2. Anti-Windup compensator 19
3.5. Sliding mode control 20
3.5.1. Sliding mode controller 21
3.5.2. Chattering 23
3.6. Longitudinal tire force observers 24
3.6.1. Sliding mode observer 24
3.6.2. Kalman filter 25
3.6.3. Simulation analysis of proposed observer designs 27
4. CO-SIMULATION ENVIROMENT WITH AVL VSM™ AND MATLAB/SIMULINK® 32
4.1. Vehicle model 32
4.2. Electric motor brake actuator 34
4.3. Brake torque distribution 35
4.4. Downsampling 36
4.5. Torque difference limiter 36
5. TEST MANEUVERS AND SIMULATION RESULTS 38
5.1. Key performance indicators 39
5.2. Test maneuver results for the case of EMBs 41
5.2.1. μ - High 41

5.2.2. μ - Low ... 43
5.2.3. μ - High to μ - Low ... 45
5.2.4. μ - Low to μ - High ... 47
5.2.5. μ - Step ... 49
5.2.6. μ - Split ... 51
5.3. Relative comparison ... 53
5.4. Comparison of proposed ABS controlled EMBs and EMs and conventional ABS ... 57
5.4.1. μ - High ... 57
5.4.2. μ - Low ... 59
6. CONCLUSION ... 62
LITERATURE ... 64

LIST OF FIGURES

Figure 1. Hydraulic ABS [1] 1
Figure 2. Hydraulic pressure hysteresis [2] 2
Figure 3. Brake systems time response [3] 3
Figure 4. Conventional electromechanical brake mechanism [4] 6
Figure 5. Electromechanical brake mechanism [3] 6
Figure 6. Brake actuation [3] 7
Figure 7. Model types [5] 8
Figure 8. EMB actuator dynamics 10
Figure 9. Hammerstein-Wiener model 11
Figure 10. Nonlinear model and transfer function response 11
Figure 11. Nonlinear model and transfer function response test 12
Figure 12. Slip-tractive coefficient curve [9] 14
Figure 13. Slip-tractive coefficient curve for various surfaces [10] 14
Figure 14. Pacejka tire model [11] 15
Figure 15. Wheel dynamics [9] 16
Figure 16. Vehicle speed gain scheduling 19
Figure 17. Gain Scheduling controller with anti-windup compensator 20
Figure 18. Sliding mode observer estimation 28
Figure 19. Kalman filter estimation 29
Figure 20. Sliding Mode Observer error 29
Figure 21. Kalman Filter error 30
Figure 22. Co-simulation environment 32
Figure 23. VW e-Golf 2017[17] 33
Figure 24. Electric motor characteristics 34
Figure 25. Braking torque allocation flowchart 35
Figure 26. Downsampling 36
Figure 27. Torque difference limiter 36
Figure 28. μ-High Gain PI Scheduling 41
Figure 29. μ-High Sliding Mode Control 42
Figure 30. μ-Low Gain PI Scheduling 43
Figure 31. μ-Low Sliding Mode Control 44
Figure 32. μ-High to μ-Low friction coefficient change 45
Figure 33. μ-High to μ-Low Gain Scheduling PI 45
Figure 34. μ-High to μ-Low Sliding Mode Control 46
Figure 35. μ-Low to μ-High friction coefficient change 47
Figure 36. μ-Low to μ-High Gain Scheduling PI 47
Figure 37. μ-Low to μ-High Sliding Mode Control 48
Figure 38. μ-Step friction coefficient change 49
Figure 39. μ-Step Gain Scheduling PI 49
Figure 40. μ-Step Sliding Mode Control 50
Figure 41. μ-Split friction coefficient change 51
Figure 42. μ-Split Gain Scheduling PI 51
Figure 43. μ-Split Sliding Mode Control 52
Figure 44. μ-Split yaw motion comparison 52
Figure 45. μ-High KPI relative comparison 54
Figure 46. μ-Low KPI relative comparison 54
Figure 47. μ-High to μ-Low KPI relative comparison 55
Figure 48. μ-Low to μ-High KPI relative comparison 55

Figure 49. μ-Step KPI relative comparison 56
Figure 50. μ-Split KPI relative comparison 56
Figure 51. μ-High with conventional ABS system (real measurements) 58
Figure 52. μ-High with Gain Scheduling PI ABS controller 58
Figure 53. μ-High comparison of stopping distances 59
Figure 54. μ-Low with conventional ABS system (real measurements) 60
Figure 55. μ-Low with Gain Scheduling PI ABS controller 60
Figure 56. μ-Low comparison of stopping distances 61

LIST OF TABLES

Table 1. Model type description 9
Table 2. Gain Scheduling PI controller parameters 20
Table 3. Sliding Mode Control parameters 23
Table 4. Observer errors 31
Table 5. Vehicle model parameters 33
Table 6. Test maneuver descriptions 39
Table 7. μ-High KPI comparison 42
Table 8. μ-Low KPI comparison 44
Table 9. μ-High to μ-Low KPI comparison 46
Table 10. μ-Low to μ-High KPI comparison 48
Table 11. μ-Step KPI comparison 50
Table 12. μ-Split KPI comparison 53

LIST OF SYMBOLS

Symbol	Unit	Description
A	m^2	Frontal area of a vehicle
B	N	Longitudinal tire force unceartainty
BD	m	Braking distance
B_x	-	Tire stiffness factor
c_w	-	is the air resistance factor
C_x	-	Form factor
D_x	-	Maximum adhesion value
E	-	Eigenmatirx
E_x	-	Curvature factor
f	-	Rolling resistance factor
F_x	N	Longitudinal force on a wheel
F_z	N	Vertical force on a wheel
$\hat{F}_x$	N	Estimated longitudinal force
h	ms	Sampling time
i	-	Index of separate wheel
IPV	deg	Integral pitch varation
IYV	deg	Integral yaw varation
J	kg m^2	Rotational inertia of a wheel
k	-	Switching gain
K_f	-	Anti-windup factor
K_I	-	Integrator gain
K_k	-	Kalman gain
K_P	-	Proportional gain
m	kg	Vehicle mass
M	-	Friction constant
MD	m/s^2	Mean deceleration
MSE	-	Maximum slip error
P_k	-	Covariance matrix error
Q	-	Process noise covariance matrix
r	m	Radius of a wheel
R	-	Measurement noise covariance matrix
s	-	Sliding surface
SE	-	Slip error
$S_{x,v}$	-	Vertical offset
t	s	Time
T_b	Nm	Braking torque

T_d	Nm	Drive torque
T_f	s	Time constant
u	Nm	System input
u_{eq}	Nm	Equivalent system input
v_k	-	Measurement noise
v_x	m/s	Vehicle longitudinal speed,
$\dot{v}_x$	m/s^2	Vehicle deceleration
$\bar{\dot{v}}_x$	m/s^2	Mean vehicle deceleration
V	N	Friction tire force
w_1	-	Random walk signal
w_2	-	Unmeasured process disturbance
W_f	-	Low-pass filter
x	-	State vector
y	rad/s	System output
α	rad	Slip angle
η	-	SMC tuning parameter
λ	-	Wheel slip
$\dot{\lambda}$	-	Wheel slip derivative
λ_{ref}	-	Reference wheel slip
μ	-	Road tire friction coefficient
μ_G	-	Sliding friction coefficient
μ_H	-	Maximum friction coefficient
ρ	kg/m^3	Air density
τ	Nm	Sum of brake and drive torques
$\dot{\phi}$	deg/s	Pitch rate
$\dot{\psi}$	deg/s	Yaw rate
ω	rad/s	Angular velocity of a wheel
$\dot{\omega}$	rad/s^2	Angular acceleration of a wheel
$\hat{\dot{\omega}}$	rad/s^2	Estimated angular acceleration of a wheel

LIST OF ABBREVIATIONS

Abbreviation	Description
ABS	Anti-lock braking system
BBW	Brake-by-wire
ECU	Electronic control unit
EMB	Electromechanical brake
ESP	Electronic stability program
HW	Hammerstein-Wiener
KPI	Key performance indicator
PI	Proportional-integral
SMC	Sliding Mode Control

SAŽETAK

Poboljšanje voznih karakteristika i sigurnosnih sustava jedna je od glavnih tema u automobilskoj industriji. Potražnja tržišta i novi rigorozni zakoni tjeraju proizvođače automobila na razvoj novih i unapređenje već postojećih sustava u svrhu podizanja sigurnosti i kvalitete iskustva vožnje automobila. Jedan od pionirskih sustava je i ABS (eng. *Anti-lock braking system*), kojemu je glavni cilj da se prilikom jakog i agresivnog kočenja spriječi tendencija blokiranja kotača te time ostvari kratki zaustavni put te zadrži visoki stupanj upravljivosti i stabilnosti za zaobilaženje mogućih prepreka. ABS sustavi su se s vremenom sve više unapređivali, zahvaljujući razvoju novih tehnologija, a i zahvaljujući iskustvu i dubljem razumijevanju problematike kočionih sustava. Unatoč tome konvencionalni ABS sustavi imaju određene nedostatke koji proizlaze iz samog dizajna. Glavni nedostatci poput sporijeg uključivanja ABS-a prilikom hladne kočione tekućine, histereza kočionog pritiska, jako vibriranje kočione pedale uslijed otvaranja i zatvaranja ABS ventila te nemogućnost održavanja klizanja kotača u optimalnoj radnoj točci i dalje su prisutni u današnjim vozilima. Ovom problemu pokušava se doskočiti primjenom električnih kočionih sustava (engl. *brake-by-wire* systems). Kod njih ne postoji mehanička ili hidraulička veza između kočione pedale i samih kočnica, već se zahtjev za kočenjem šalje od upravljačke jedinice do elektromehaničkog aktuatora. Upravo je tema ovog rada ispitati izvedivost takvih sustava uparenih s ABS upravljanjem na električnim vozilima, kako bi se postiglo još brže, tj. optimalno kočenje u smislu skraćenja zaustavnog puta i poboljšanja upravljivosti prilikom kočenja. Prvo se predstavlja način modeliranja elektromehaničke kočnice unutar MATLAB/Simulink® okruženja. Zatim se, uz pomoć četvrtinskog modela automobila i dinamike kotača izvode jednadžbe na kojima se temelje dvije arhitekture regulatora i pomoćni algoritmi koji su razmatrani u ovom radu. Pregledom literature uočeno je da se za ABS upravljanje e-kočnicama najčešće koriste PI regulatori s planiranom adaptacijom pojačanja te regulatori zasnovani na kliznim režimima te su isti razmatrani u ovom radu. Nadalje je prikazan kooperativni simulacijski model AVL VSM™-a i MATLAB/Simulink®-a te način na koji su ovi programski paketi povezani. Naposlijetku prikazan je model vozila za dva različita rasporeda elektromehaničkih kočnica i elektromotora, uz pomoć kojeg se ispituje robusnost samih regulatora na testnim manevrima uobičajenim za ispitivanje kočionih sustava.

Ključne riječi: Sustav kočenja uz sprečavanje blokade kotača, *elektromehanička kočnica, PI regulator, planirana adaptacija, regulator zasnovan na kliznim režimima, AVL VSM™*

SUMMARY

One of the main topics in automotive industry is improvement of vehicles driving characteristics and development of safety systems. Market demand and new rigorous legislation are forcing car manufacturers on further developing of already existing systems with the goal of improving safety and overall driving experience. One of the pioneering systems is ABS (*Anti-lock braking system*), which has a main goal of preventing tendency of wheel lock during emergency braking, which in the end shortens the braking distance. Also, stability and manoeuvrability during braking must be left, so possible obstacles can be avoided. ABS systems have improved, owing to the development of new technologies, but also owing to acquired experience and deeper understanding of braking systems. Of course, conventional ABS systems have disadvantages which are resulting from its design. Main disadvantages like slower actuation time when the braking fluid is cold, brake pressure hysteresis, furious brake pedal oscillations during ABS engage-release valve switching and lastly the inability of keeping the tire slip in optimal working point are still present in current vehicles. These problems are trying to be solved with *brake-by-wire* systems. *Brake-by-wire* implicates that there is no mechanical or hydraulic connection between the brake pedal and the actuator, but instead the braking demand is sent over the micro-controller to the electromechanical actuator. The main goal of this thesis is to proof feasibility of this kind of systems paired with ABS control on electric vehicles to achieve faster actuation times, which results in shortening of braking distance and better vehicle manoeuvrability. First, model of the electromechanical brakes is presented in MATLAB/Simulink® environment. Then, equations have been derived with the help of quarter car model and wheel dynamics, on which two control architectures and observers are based. Browsing through literature it can be noticed that for ABS control of *brake-by-wire* systems, *Gain Scheduling PI* and *Sliding mode control* architectures have been used and have proven to be robust, so the mentioned controllers are presented in this work. Later, co-simulation model of AVL VSM™ and MATLAB/Simulink® has been presented and how these software packages are connected. Finally, two different electromechanical and electric motor brake configuration layouts are examined and how the ABS controllers are performing paired up with said brakes on typical braking test manoeuvres.

Key words: *Anti-lock braking system, brake-by-wire, electromechanical brake, Gain Scheduling PI control, Sliding mode control, AVL VSM™*

PROŠIRENI SAŽETAK

Cilj ovog diplomskog rada jest provesti simulacijsku analizu i ocijeniti izvedivost sustava ABS upravljanja elektromehaničkom kočnicom i elektromotorom u električnim vozilima unutar AVL programskog paketa VSM™ i programskog paketa MATLAB/Simulink®.

Konvencionalni hidraulični ABS sustavi često zbog sporijeg odziva nemaju željene performanse prilikom kočenja u nepovoljnim uvjetima na cesti zbog nemogućnosti održavanja klizanja kotača u optimalnoj radnoj točci. Spomenutom i sličnim nedostatcima želi se priskočiti primjenom električnih kočionih sustava. Kod njih ne postoji mehanička ili hidraulička veza između kočione pedale i samih kočnica, već se zahtjev za kočenjem šalje od upravljačke jedinice do elektromehaničkog aktuatora. Upravo je i tema ovog rada ispitati izvedivost takvih sustava u paru s ABS upravljanjem na električnim vozilima te usporediti performanse s konvencionalnim sustavom. Izraditi će se jednostavni modeli elektromehaničkih aktuatora te modeli upravljanja kočnicama sa električnim sučeljem. Simulacijskom analizom provjeriti će se performanse dvije konfiguracije razmještaja elektromehaničkih kočnica i elektromotora. Uz pomoć provedenih testnih manevara utvrditi će se robusnost i potencijal predloženog sustava.

Ovaj rad je organiziran u šest poglavlja s zaključkom, čiji sadržaj je sažet kako slijedi.

Poglavlje 1 - 'Uvod' – U uvodu je objašnjena motivacija koja stoji iza istraživanja u ovom radu te osim toga objašnjen je rad konvencionalnih hidrauličnih ABS sustava. Rad konvencionalnih hidrauličkih sustava uspoređen je sa radom *brake-by-wire* sustava i naposlijetku su se opisale karakteristike elektromehaničkih kočnica i prednosti istih naspram onih hidrauličkih.

Poglavlje 2 - 'Model elektromehaničkih kočnica' – U ovom poglavlju opisane su karakteristike korištene elektromehaničke kočnice te napredak u razvoju istih u odnosu na prijašnje izvedbe elektromehaničkih kočnica. Opisan je i način pristupa modeliranju kočnica u simulacijskom okruženju i razlog odabira takvog pristupa.

Poglavlje 3 - 'Regulacija klizanja kotača' – U ovom poglavlju postavljena je jednadžba dinamike četvrtinskog modela vozila, odnosno jednadžba dinamike pojedinog kotača vozila.

Na temelju tih jednadžbi, izvedena su dva ABS regulatora različitih arhitektura. Izveden je PI regulator s planiranom adaptacijom pojačanja te regulator zasnovan na kliznim režimima. Regulator zasnovan na kliznim režimima, za regulaciju klizanja kotača koristi iznos uzdužne sile kotača na podlozi te potrebno je bilo razviti algoritam koji dovoljno precizno procjenjuje iznos spomenute sile. Također, izvedena su dva algoritma za procjenu uzdužne sile. Jedan se algoritam također temelji na kliznim režimima, dok je drugi izveden u obliku Kalmanovog filtra. Na kraju poglavlja dana je usporedba rada i usporedba preciznosti tih algoritama.

Poglavlje 4 - 'Kooperativno simulacijsko okruženje AVL VSM™-a i MATLAB/Simulink®-a – U ovom poglavlju prikazuje se kooperativno simulacijsko okruženje između AVL VSM™-a i MATLAB/Simulink®-a te ulazni i izlazni signali koje spomenuti programi izmjenjuju međusobno. Pokazane su i konfiguracije rasporeda kočnica na kotačima, odnosno koriste li se u svrhu kočenja samo elektromehaničke kočnice ili se elektromehaničke kočnice koriste u paru sa električnim motorima koji prilikom kočenja rade u generatorskom načinu rada.

Poglavlje 5 - 'Testni manevri i rezultati simulacija' – U ovom su poglavlju objašnjeni testni manevri na kojima će se ispitivati rad i robusnost ABS regulatora te je postavljena verifikacijska metrika. Prikazani su rezultati testnih manevara i analizirane su karakteristike pojedinog regulatora uz pomoć spomenutih rezultata.

Poglavlje 6 - 'Zaključak' – Unutar zaključka dana su zapažanja koja su se prikupila prilikom izrade rada te koja su izvedena iz rezultata. Također predložena su daljnja poboljšana i mogući pravci na kojima rad može nastaviti.

1. INTRODUCTION

This thesis is done in cooperation with AVL-AST d.o.o. from Zagreb and AVL list GmbH from Graz with the purpose of developing an ABS controller that is going to act on electromechanical brakes and electric traction motors of electric vehicles.

1.1. Motivation

ABS (*Anti-lock braking system*) is a safety anti-skid braking system used on land vehicles such as cars and motorcycles, but it is also used on aircrafts. Main goal of the ABS is to prevent the wheels from locking up during braking and to maintain greatest possible traction to shorten the stopping distance of a vehicle. Also, because the wheels are not locking up there is still some of the maneuverability left. ABS systems have been used for 30-35 years in the automotive industry and with the progress of the technology, equipment and with gaining of experience the ABS systems have become increasingly sophisticated and effective. Currently most of production vehicles are equipped with an electronically-controlled hydraulic ABS which is shown in Figure 1.

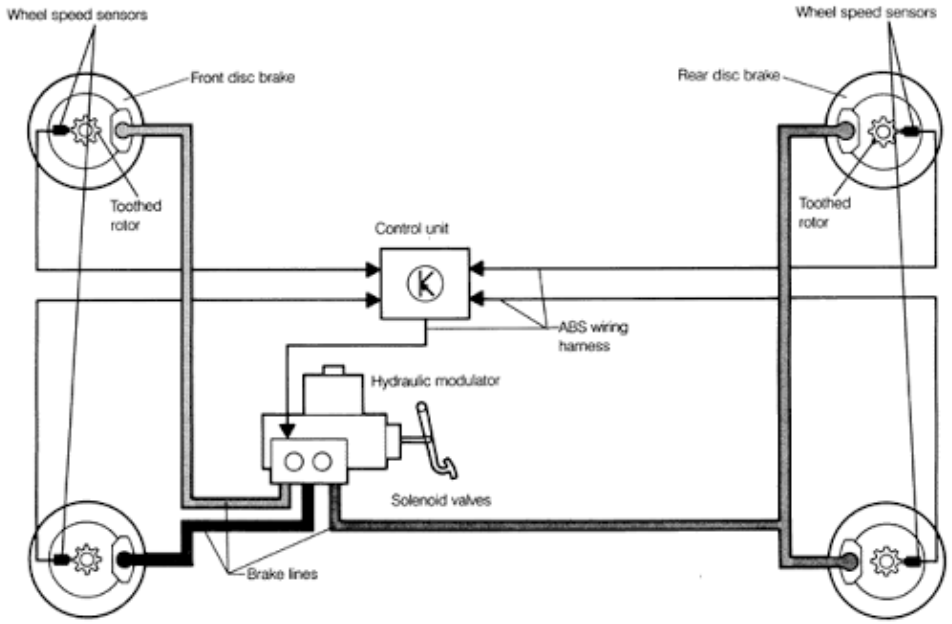

Figure 1. Hydraulic ABS [1]

Typically ABS includes a central electronic control unit (ECU), four wheel speed sensors, and at least two hydraulic valves within the brake hydraulics. The ECU constantly monitors the rotational speed of each wheel; if it detects the wheel rotating significantly slower than the speed of the vehicle, a condition indicative of impending wheel lock, it actuates the valves to reduce hydraulic pressure to the brake at the affected wheel, thus reducing the braking torque

on that wheel; the wheel then turns faster. Conversely, if the ECU detects a wheel turning significantly faster than the others, brake hydraulic pressure to the wheel is increased so the braking torque is reapplied, thus slowing down the wheel.

But, there are some disadvantages of conventional hydraulics systems. Conventional ABS cannot keep the tire slip in optimal working point, yet the tire slip value is oscillating around the setpoint value. Also, when the braking demand pressure is low and the braking fluid in the system is cold, ABS systems can be very slow. Also, pressure-hysteresis leads to unpredictive behavior of hydraulic brakes. The way the hydraulic pressure is increasing when pressing the brake pedal, and the way the brake pressure in decreasing when releasing the brake pedal is not the same. For easier understanding, pressure hysteresis is presented in Figure 2.

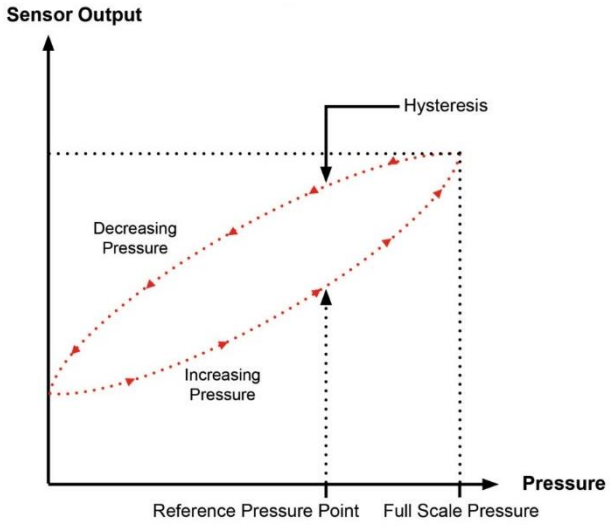

Figure 2. Hydraulic pressure hysteresis [2]

Furthermore, during engage-release valve switching the pedal position is oscillating and a loud hammering noise of brakes can be heard which sometimes leads to driver lifting from brake pedal in panic braking situations.

As previously mentioned, automotive industry is constantly improving and with the new technologies it is trying to improve the safety standards in vehicles. In terms of braking systems there has been a lot of research going on with *brake-by-wire* technology for the past two decades. *Brake-by-wire* implies that there are no mechanical or hydraulic connections between the brake pedal and the brake actuators. The sensed driver brake command is communicated through a micro-controller to the actuator. This technology replaces traditional components such as the pumps, hoses, fluids and master cylinders with electronic sensors and actuators. It can be easily concluded that these brakes are easier to maintain because of the fewer parts and easier to control than the hydraulic ones. One the examples of *brake-by-wire* systems are

electromechanical brakes (or shorter EMBs) which are using electric motors as actuators for moving mechanisms that are pressing disc pads on brake discs. Mechanisms can vary from gear driven ball screws [4] to lever assemblies [3].

Potential advantages of EMBs over hydraulic brakes are numerous. Assistance functions like ABS, ESP an etc. can be realized by software and sensors without additional hydraulic components. Furthermore, it is easier to adapt these functions due to the electrical interface instead of hydraulic one.

In Figure 3 various brake responses to step torque command are shown, from electro-hydraulic IBC brake to conventional hydraulic brakes. It is seen that the electromechanical brake has the fastest reaction, due to the fast response of the electric motor actuator that is implemented in the brake.

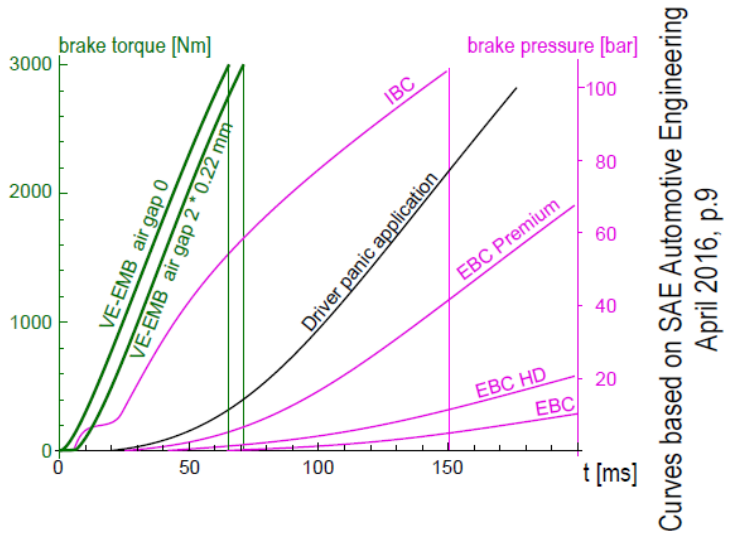

Figure 3. Brake systems time response [3]

Electric motor is a component that is easy to control, and that is the reason why it is being used as actuator in electromechanical brakes. Controllability and predictiveness of electromechanical brakes, makes them good candidates for ABS control, specifically in keeping the tire slip in desired operating range with almost no oscillations, thus shortening the braking distance.

Economy of electromechanical brakes is also one of the advantages. Firstly, they do not require hydraulic fluid for their operation. Therefore, they are easier to set up correctly, and are less harmful to the environment. Previously mentioned problems like pressure-hysteresis, brake and pedal pulsation etc. are going be eliminated because the pedal is not directly connected to the brake. But, lack of the redundant connection between the brake pedal and brake itself can also bring a disadvantage, in a standpoint of drivers brake pedal feel which has to be achieved

in other ways. Another disadvantage of electromechanical brakes is that they cannot be used on electric vehicles on their own, yet they have to be used in pair with conventional hydraulic brakes due to safety concerns, regarding the power supply failure etc. Nevertheless, the controllability and predictability are advantages of *brake-by-wire* systems that can be exploited, and their potential is seen in transient road conditions and similar situations.

In second chapter model of electromechanical brake that is going to be used in this simulation studies, is presented and how the dynamics of the brake is modeled. After that in third chapter proposed ABS control architectures are presented and the wheel dynamics is shown on which these architectures are based on. In fourth chapter a co-simulation environment between AVL VSM™ and MATLAB/Simulink® is shown. The ABS control and brake actuator dynamics is modeled in MATLAB/Simulink®, whilst vehicle, tire, driver model and test maneuvers are parametrized in AVL VSM™. In fifth chapter test maneuvers used for performance assessment of built up ABS controllers are presented. After that, results and comparisons of ABS controllers are presented, and the feasibility of the mentioned controllers is proven which is the main goal of this thesis. Finally, conclusion is given in the last chapter.

2. ELECTROMECHANICAL BRAKE MODEL

The main goal of this thesis is to design a robust anti-lock braking system controller that will act upon electromechanical brakes. To design such a controller, it is necessary to know how the system behaves in variety of cases, from braking when the surface of the brake disc is cold to cases when the brakes are hot and are used frequently. Brake modeled in this simulation studies, have a lot of parameters that have great effect on brake response, maximum braking torque etc. These parameters are sometimes complicated to be determined and are making modeling of the electromechanical brake in simulation environment very hard. Thorough testing and investigation must be conducted to find how these parameters are changing and how they are affecting the system in whole, but these processes are time consuming and often the model can be described in other ways. Later in the chapter the process of electromechanical brake modeling in simulation environment will be shown, but beforehand basic working principles and characteristics of electromechanical brakes will be explained.

2.1. Basic working principle and characteristics of electromechanical brakes

Electromechanical brakes are systems that entirely rely on electromechanical actuators and control systems to operate them. In most cases the electric actuator is the electric motor which drives a mechanism which afterwards moves the pads that brake the rotating disc. As previously mentioned in chapter 1, electromechanical brakes use a set of gears that turn a ball screw and effectively rotational motion is converted into linear motion. Ball screw moves a piston which finally pushes on a brake pad which causes it to press on the disc brake [4]. The mentioned mechanism of the conventional electromechanical brake can be seen in Figure 4. It must be noted that motor power and transmission ratio are constrained with the size of the motor and the whole transmission, because both mentioned parts have to be placed in the brake housing, that is afterwards mounted on a wheel hub and placed into a wheel arch. Size and mass play a big part in designing such a system, especially from the standpoint of increased suspension unsprung masses, which affects the driving capabilities and ride comfort of a vehicle.

Electromechanical brake used in this simulation studies [3] also uses electric motor for driving the mechanism, which isn't different from any other market available electromechanical brakes [4], but there is a difference in the pad pressing mechanism.

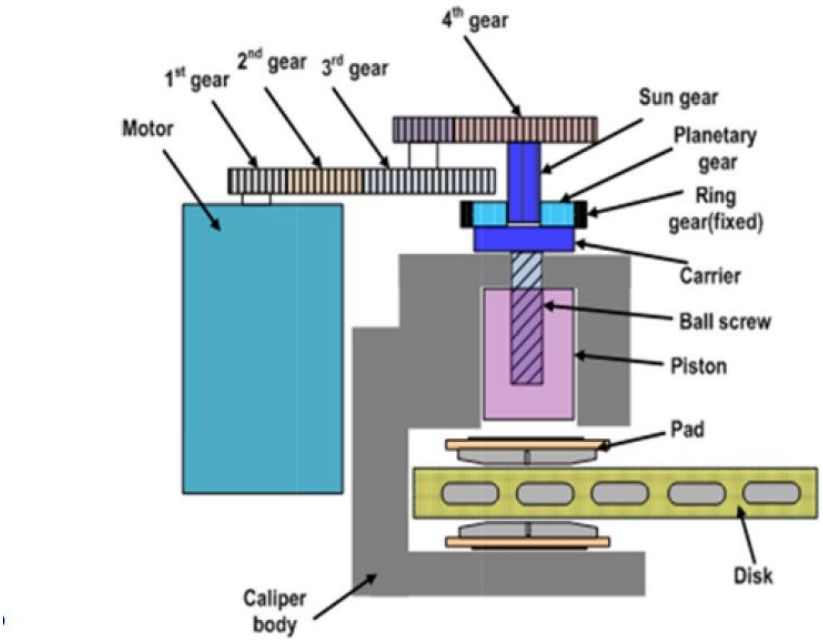

Figure 4. Conventional electromechanical brake mechanism [4]

Electromechanical brake used in this simulation studies, does not use the gear mechanism. Instead, it is comprised of mechanism that has levers and an actuation disk or „actuation snail "as it is called. The mentioned components can be seen in Figure 5.

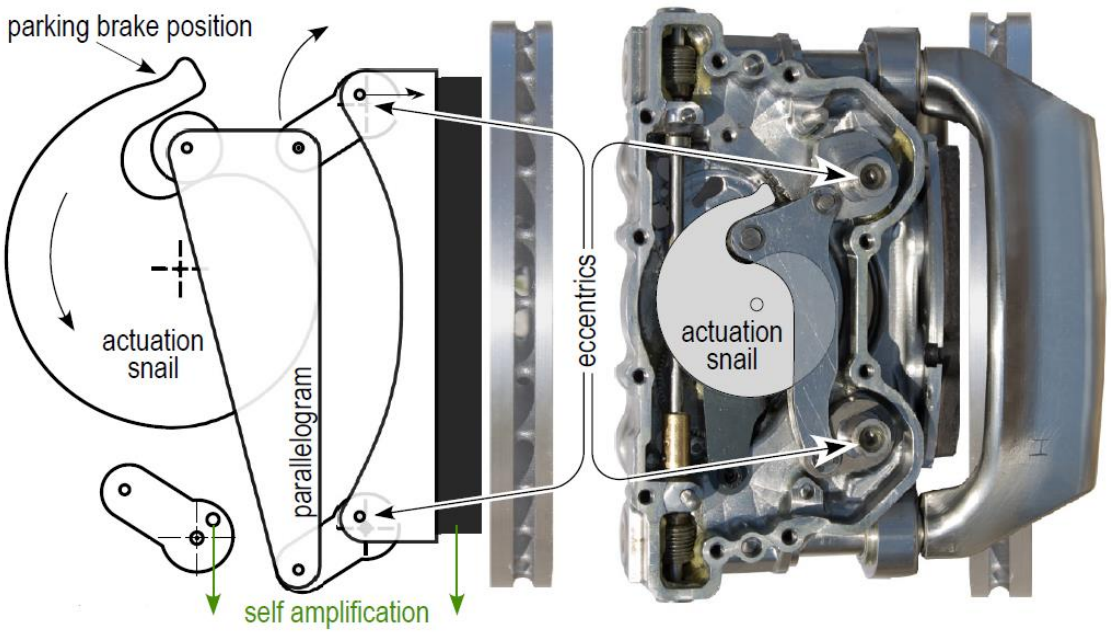

Figure 5. Electromechanical brake mechanism [3]

Electric motor is directly connected to the actuation snail, and when the actuation snail is turned anti-clockwise by the motor, its turning motion moves a parallelogram that is connected to the

pad via levers. The levers then move the pad which the presses on the brake disc. Whole actuation process can be seen on Figure 6.

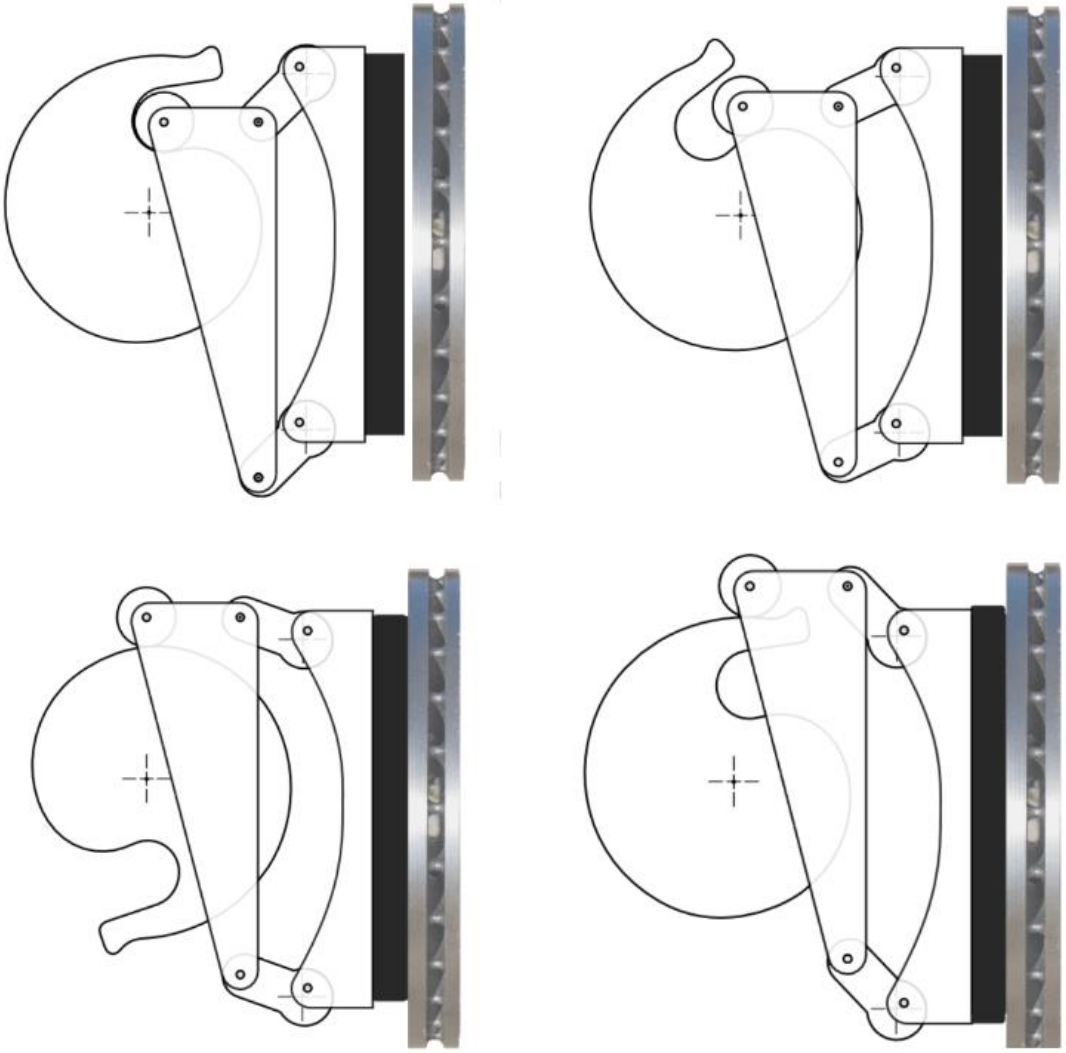

Figure 6. Brake actuation [3]

The mechanism transmission ratio of the brake used in simulation studies (Figure 5) is greater than the transmission ratio of the conventional brake. Therefore, to achieve the same braking torque as the first brake, the later brake will achieve it with less actuator motor torque. In the aftermath this means that smaller sized motor with less torque can be used for actuation. Finally brake housing is smaller and it weighs less which benefits driving comfort.

At the beginning the actuation snail radius is small, so the response is quite rapid, but as snail radius changes with motor angle, the braking torque characteristic will be nonlinear, and this presents a problem when it comes to the control of the brake. By adjusting the shape of the actuation snail, actuation timing and maximum motor torque can be balanced, dependently on the use and scenarios in which the brake is going to be used [3].

2.2. Theoretical and experimental mathematical models

Mathematical models are an essential part for simulation and design of control systems. The purpose of the mathematical model is to be a simplified representation of reality, to mimic the relevant features of the system being analyzed. Two main categories of mathematical modeling can be distinguished: theoretical and experimental modeling. In theoretical modeling, the system is described using equations derived from physics, mainly differential equations of the first order. There are almost no uncertainties to how the system functions and all parameters that are necessary for good description of the model are known. This kind of systems are often linearized because of the simplicity. For example, spring characteristic in suspension systems is often linearized. Systems which are modeled entirely based on physical principles are called white-box models.

In many cases, the mathematical model of the system, ends up complicated and requires simplification. Experimental modeling, also called *system identification*, is based on measurements. The mathematical model of the system is derived from several sets of measurements, each recording the system's response (output) for different inputs. System which are modeled entirely based on experimental data are called black-box models. This means that the input and output of the system are known, but not the process behind it.

Experimental modeling could be the right method for modeling due to the various reasons. If the system is complex, deriving mathematical equations can be very hard. Quite often most of the parameters used in the mathematical equations are not know, so the overall behavior of the modeled system is uncertain. In addition, not all physical behavior of the system is known and capturing some of the characteristics is not an easy task.

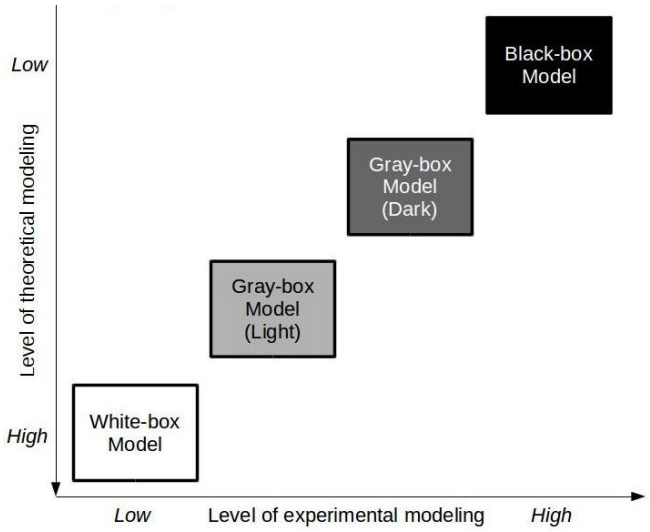

Figure 7. Model types [5]

Table 1. Model type description

Model type	Characteristics	**Model description**
White-box	• known parameters • known physical laws	• Linear and nonlinear equations
Light-gray-box	• some physical laws are known • model structure known • unknown parameters	• Linear and nonlinear equations with parameter estimations • Transfer functions with parameter estimations
Dark-gray-box	• some of the physical governing laws known • model structure unknown • parameters unknown	• Neural or fuzzy models
Black-box	• model structure unknown • parameters unknown	• Artificial neural networks

2.3. System identification of EMB dynamics

The easiest approach to this problem is to model the electromechanical brakes as a dark-gray or a black-box model. Input and output signals need to be measured, so the model of the electromechanical brake can be estimated.

EMBs have been mounted on a testbed to get a variety of measurement data and to roughly identify the behavior of the brake. Various tests have been conducted, but because of the simplicity of identifying the brake dynamics, brakes response to step torque command will be used as a basis. Proposed ABS controller will have an output of a demanded braking torque and will serve as an input to identified EMB model. The output of the model will be actual braking torque. As in this thesis the actuator dynamics represents a response and simple replication of EMB behavior, a simple transfer function will be estimated with MATLAB® System Identification Toolbox. EMB braking torque response is shown on Figure 8. As mentioned, the brake itself has a nonlinear behavior, but mostly the brake performs in linear region, so for this work the nonlinear behavior will be linearized.

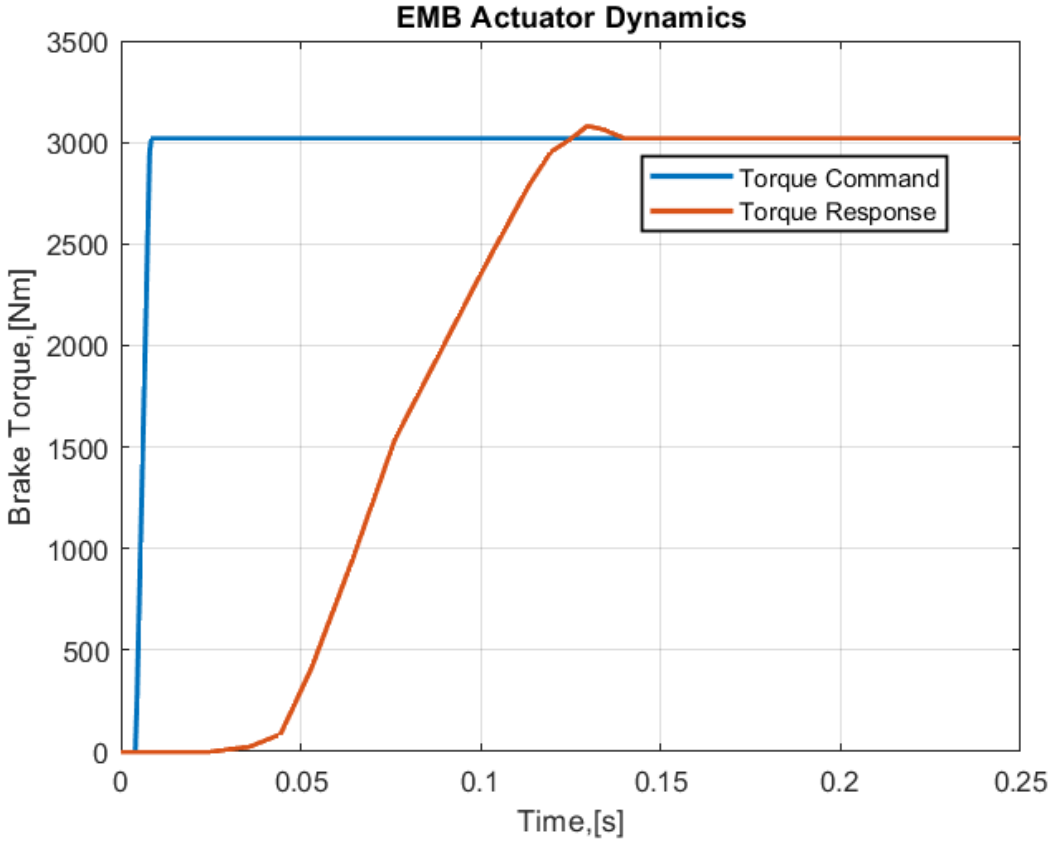

Figure 8. EMB actuator dynamics

Looking at the measured EMB step torque response in Figure 8, it resembles the step response of second order transfer function. With this knowledge the goal will be to estimate parameters of the second order transfer function with high fit percentage. Of course, System Identification Toolbox can estimate nonlinear models to a high precision fit, but the problem arises when the braking torque demand in simulation analysis isn't the same as the one used in the estimation process. In real life situations brake demand will often change quickly and the model needs to be capable of responding precisely to the given demand. Estimated nonlinear models mimic the dynamics of a system precisely in isolated cases, where input to the estimated model is always the same. If the input to the estimated nonlinear model is changed, the precision could fall to lower values. Decision to choose between estimated transfer function and nonlinear model is presented in the following Figures.

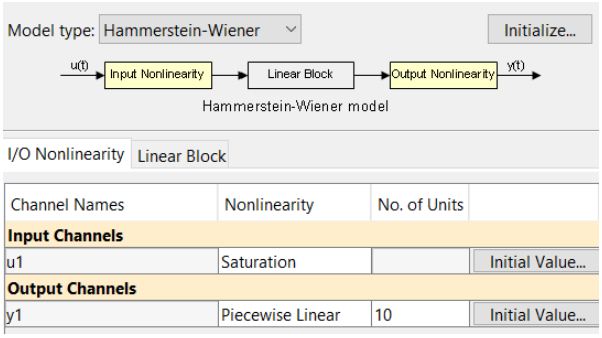

Figure 9. Hammerstein-Wiener model

For estimation of the nonlinear model, in System Identification Toolbox, Hammerstein-Wiener model is chosen, and estimation setup for step torque command and measured step torque response is shown in Figure 9. Input nonlinearity of Hammerstein-Wiener model is defined as saturation nonlinearity [6], whilst the output nonlinearity is defined as piecewise linear approximation [7]. Estimation fit of HW model returns a value of 98,64%. For an estimation of second order transfer function the same step torque command and measured step torque response shown in Figure 9 are used. In estimation process of second order transfer function number of poles was set at 2, and number of zeros was set at 0. It returned an estimation fit of 92,95 %. The responses of the nonlinear and transfer function models are shown in Figure 10.

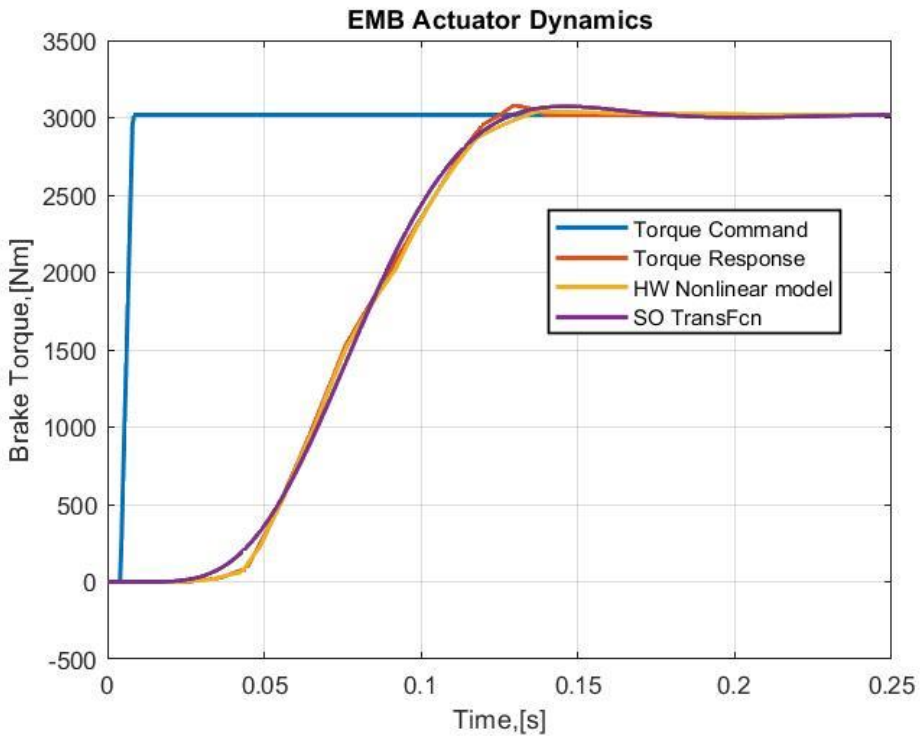

Figure 10. Nonlinear model and transfer function response

The transfer function has a good fit in the linear range of the response but lacks the precision when reaching the demanded value. The nonlinear model resembles the original torque response data throughout the graph, but if the form of input step torque demand is changed, the Hammerstein – Wiener model will become unprecise. New step torque command has been given, the command of 3000 Nm that lasts for 0,5 s, after that command of 0 Nm is given for 0,5 s, and finally again the command torque is equal to 3000 Nm. As assumed the performance of the nonlinear model has lowered, and it is seen between 0,5 s and 1 s that output of nonlinear is equal to 600 Nm instead of 0 Nm. However, the estimated model of second order transfer function still manages to perform in transient conditions as expected. Same behavior is exhibited throughout the new step torque command. Therefore, the estimated transfer function will serve as an EMB actuator dynamics in this simulation analysis. Results are presented in Figure 11.

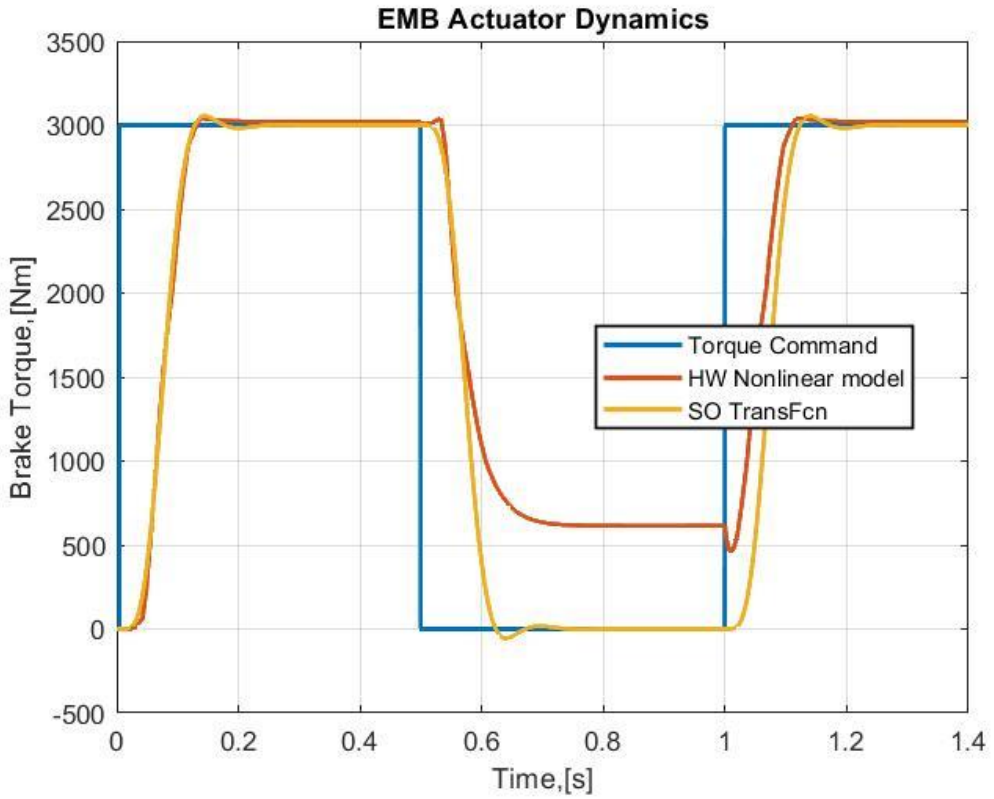

Figure 11. Nonlinear model and transfer function response test

3. WHEEL SLIP CONTROL

The wheel slip is according to the typical non-linear longitudinal force characteristic (slip curve) kept in the optimal range to maximize the braking force and thus minimize the braking distance.

One of the main reasons is the nonlinearities and uncertainties that are involved. The biggest one is tire as its behavior is highly nonlinear, specifically the friction between the tire and road. Design of the wheel slip control system will not be strictly tied to one type of tire and one vehicle geometry, so also with that in mind, parameters like vehicle mass, center of gravity height, distance from center of gravity to front and rear axle etc. present a type of uncertainty.

3.1. Tire modeling

In general, because of tire deformation and because of traction and braking forces exerted on the tire, the vehicle velocity is not equal to wheel speeds. If the radius of the braked wheel is r and the angular velocity is ω,the longitudinal slip coefficient λ can be defined as [8]:

$$\lambda = \frac{\omega r - v_x}{\max\{v_x, \omega r\}} = \frac{\omega r \cdot \cos(\alpha) - v_x}{\max\{v_x, \omega r \cdot \cos(\alpha)\}} \quad \textbf{(1)}$$

where α is the wheel slip angle. In vehicle dynamics, slip angle is the angle between a braked wheel's actual direction of travel and direction towards which it is pointing. Since this thesis is concentrated on braking maneuvers taking place on a straight-line, slip angle is not considered. So, the equation becomes:

$$\lambda = \frac{\omega r - v_x}{v_x} \quad \textbf{(2)}$$

The tire friction force is determined by [9]:

$$F_x = F_z \mu(\mu_H, \alpha, \lambda) \quad \textbf{(3)}$$

where $\mu(\mu_H, \alpha, \lambda)$ is the road-tire friction coefficient, nonlinear function with a typical dependence on the slip shown in Figure 12. This function depends on, slip angle α, tire slip λ and μ_H represents maximum friction coefficient between tire and road. The friction coefficient μ can span over a very wide range, but is generally a differentiable function with respect to all arguments and has the properties $\mu(\mu_H, \alpha, 0) = 0$ and $\mu(\mu_H, \alpha, \lambda) > 0$ for $\lambda > 0$. Figure 12 shows how the friction coefficient μ increases with slip λ up to a value λ_0, where it attains its maximum value μ_H. For higher slip values, the friction coefficient will decrease to a minimum μ_G where the wheel is locked and only the sliding friction will act on the wheel. The

dependence of friction on the road condition is shown in Figure 13. For wet or snow roads, the maximum friction μ_H is small and the right part of the curve is flatter.

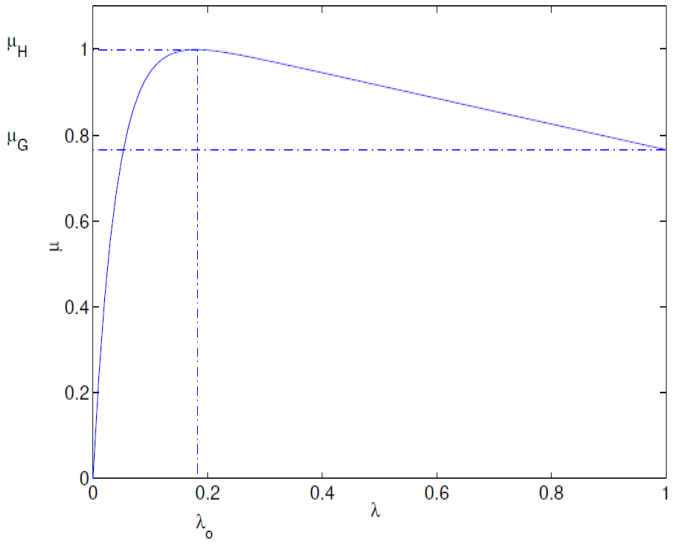

Figure 12. Slip-tractive coefficient curve [9]

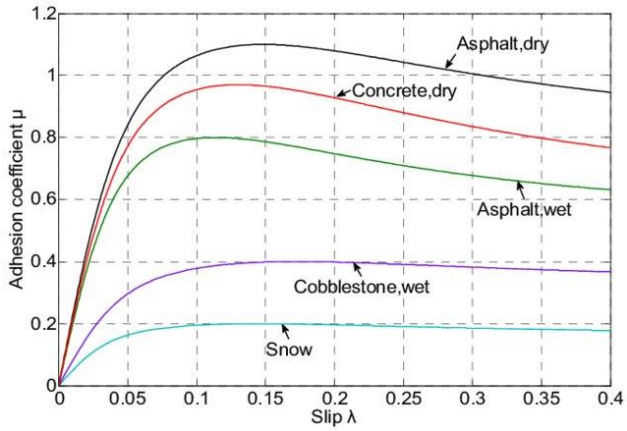

Figure 13. Slip-tractive coefficient curve for various surfaces [10]

Several tire models describing the nonlinear behavior are used in simulation studies but, Pacejka tire model which is also known as the Magic Formula is the most reputed one. It is derived heuristically from experimental data. It provides the tire/road coefficient of friction μ as a function of the slip λ by using static maps. In this study just the longitudinal vehicle dynamics is considered. Then the Magic Formula for pure longitudinal slip reads [11]:

$$F_x = D_x \cdot \sin(C_x \cdot \arctan(B_x\lambda - E_x(B_x\lambda - \arctan(B_x\lambda)))) + S_{x,v} \quad \textbf{(4)}$$

Parameters from the previous equation also have following physical meanings and are shown in Figure 14:

- D_x maximum adhesion value,
- C_x form factor which determines the shape of the maximum,
- B_x stiffness factor which determines the rise from the origin,
- E_x curvature factor, determines the unstable area of the slip curve
- $S_{x,v}$ vertical offset

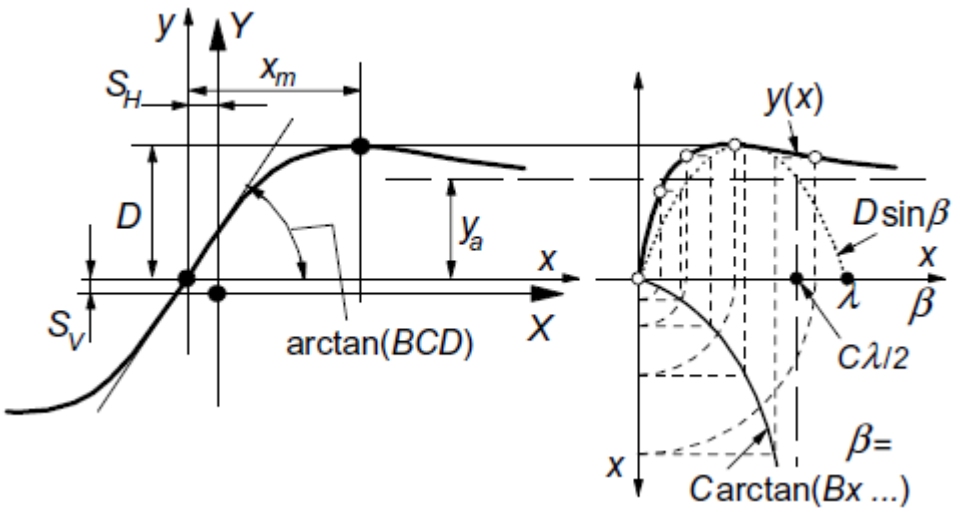

Figure 14. Pacejka tire model [11]

Pacejka tire model can be modeled with the mentioned set of parameters in AVL VSM^{TM}, and it is used because of its high precision, which is suitable for this simulation analysis work.

3.2. Problem description

Since ABS control system uses a reference value of longitudinal wheel slip, an equation that describes longitudinal vehicle dynamics will be used. For easier writing of the equations the dependencies of functions will be left out. The mentioned equation reads:

$$m \cdot \dot{v}_x = -\sum_i F_{x,i} - \sum_i f_i \cdot F_{z,i} - c_w \cdot A \cdot \frac{\rho}{2} \cdot v_x^2 \qquad \textbf{(5)}$$

where:

- F_x longitudinal force on a wheel,
- F_z vertical force on a wheel,
- f rolling resistance factor,
- c_w resistance factor,

- A frontal area of a vehicle,
- ρ air density,
- v_x vehicle longitudinal speed,
- m vehicle mass.
- i index of every separate wheel.

The air resistance and the rolling resistance that are included in the equation are not going to be considered for the controller design. This can be justified by the fact that the vehicle speed and rolling resistance are not changing much on a time scale of control, so they are considered as a slow disturbance which the controller will eliminate. Air resistance is also negligible for the investigated speed range when compared to the braking force at full deceleration. After all that concluded Equation (5) now reads:

$$m \cdot \dot{v}_x = -\sum_{i=4}^{4} F_{x,i} \tag{6}$$

During braking the wheel slip and consequently the tire longitudinal force are regulated to a desired setpoint, so the tire longitudinal force therefore remains constant on a homogeneous surface. Only with changes in the surface the longitudinal force changes its value and up until it returns to its stationary value.

The wheel dynamics itself can be described with so called quarter car model. This model consists of a vehicles single wheel, as shown in Figure 15.

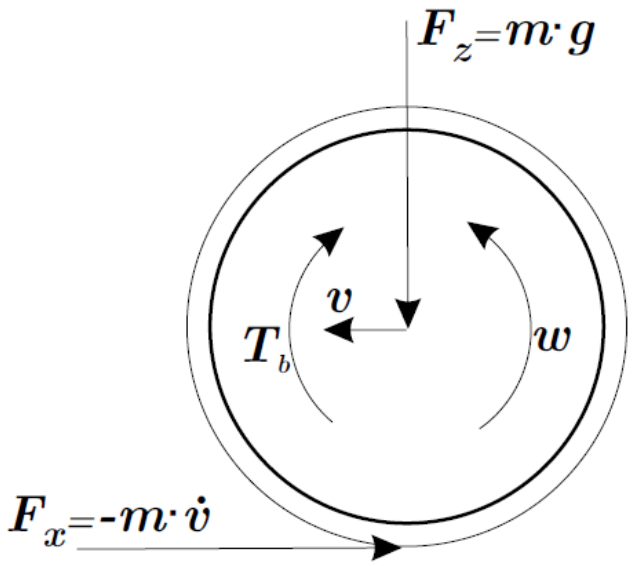

Figure 15. Wheel dynamics [9]

As in the quarter car model, only one wheel is considered, the index i can be eliminated for purpose of setting this equation. Wheel has its inertia, but also the wheel is attached to drivetrain and the rotational inertia of a drivetrain cannot be neglected. Besides of the wheel inertia, brake and drive torque act upon a wheel, and so does the longitudinal friction force F_x. With all that said the sum of moments reads:

$$J \cdot \dot{\omega} = r \cdot F_x - T_b \tag{7}$$

where:

- T_b is the braking torque,
- J is the rotational inertia of a wheel,
- $\dot{\omega}$ is the rotational acceleration of a wheel.

3.3. Slip dynamics

Equation (2) can be written as:

$$\omega = \frac{v_x}{r}(1+\lambda) \tag{8}$$

Wanted characteristic of the controlled system is that slip ratio remains constant as much it is possible. To ensure this we need to define the equation for the derivative of slip ratio λ. Derivative of Equation (8) reads [9]:

$$\dot{\omega} = \frac{\dot{v}_x}{r}(1+\lambda) + \frac{v_x}{r}\dot{\lambda} \tag{9}$$

Expressing Equation (9) in terms of slip ratio derivative yields:

$$\dot{\lambda} = -\frac{\dot{v}_x}{v_x}(1+\lambda) + \frac{\dot{\omega} r}{v_x} \tag{10}$$

Substituting Equations (6) and (7) into (10) gives the following relation:

$$\dot{\lambda} = \frac{1}{v_x}\left[\frac{r^2}{J}F_x + \frac{1}{m}(1+\lambda)F_x - \frac{r}{J}T_b\right] \tag{11}$$

Now it can be seen that the goal of the controller is to apply just enough braking torque, so the slip ratio is equal to the reference slip ratio. This can be expressed as:

$$\dot{\lambda} = 0 \tag{12}$$

Notice that the slip dynamics is highly affected by the inverse of the longitudinal vehicle speed. Because of this at low speeds, eventual deviations in braking torque have stronger effect than in high speeds. This will have an important effect on the control performance. Also, wheel inertia has effect on slip control, especially driven wheels that are connected to drivetrain, which

also has some rotational inertia. Heavier wheels slow down the slip control dynamics and this needs to be considered. Lastly as the brakes are going to be controlled separately, just one longitudinal force on a wheel is investigated for every separate wheel. The problem arises when it needs to be defined which mass m is going to be considered for the control design. For definition of wheel slip, quarter car model is used. Despite the model is call quarter car model, vehicle mass m can't be split into four equal parts for each wheel. If the brakes are mounted on the front axle and the rear axle will not be braked the vehicle mass can be split on two equal halves for each wheel. If both axles are being braked, then brake distribution factor comes in play. Typically, this factor is around ratio 2:1, so for the front wheels mass m is equal to one third of the whole mass and for the rear wheels mass is equal to one sixth of the whole mass.

3.4. Gain-Scheduling PI control

Browsing through literature it is easy to stumble upon brake-by-wire anti-lock brake controllers and the most often used principle is the proportional-integral (PI) control. In [9] and [12] a *Gain Scheduling PI* control principle is applied and tested for robustness in various conditions and it has shown good results. For this thesis a similar approach will be considered, but the approach of gain scheduling will be different.

Gain scheduling is an approach to control of non-linear systems that uses a family of linear controllers, each of which provides satisfactory control for a different operating point of the system. One or more observable variables, called the scheduling variables, are used to determine what operating region the system is currently in and to enable the appropriate linear controller. Scheduling variables are mostly the variables that do not change fast over time. As wheel and car body have a big difference in inertias the vehicle speed will change much more slowly than the wheel slip, and because of that vehicle speed is a good candidate to be used as a scheduling variable. To design such a controller the equations used in the controller design must be linearized. Equation (11) is written in following form [9]:

$$\dot{\lambda} v_x = \left[\frac{r^2}{J} + \frac{1}{m}(1+\lambda) \right] \mu F_z - \frac{r}{J} T_b \qquad \textbf{(13)}$$

To linearize the previous equation, constants α and β are introduced as [9]:

$$\beta = \left[\frac{r^2}{J} + \frac{1}{m}(1+\lambda) \right] F_z \qquad \textbf{(14)}$$

$$\alpha = \frac{r}{J} \qquad \textbf{(15)}$$

Introducing the new constants α and β into Equation (13) gives:

$$\dot{\lambda} v_x = \beta(\lambda) - \alpha T_b \quad \textbf{(16)}$$

To completely linearize the expression, nonlinear slip curve is linearized around an operating point [12]:

$$\dot{\lambda} v_x = \beta(\psi + m_i \cdot \lambda) - \alpha T_b \quad \textbf{(17)}$$

Where m_i is the slope of the tire-friction curve at the considered operating point and ψ represents the offset of the operating point. Then locally the slip dynamics is given by a first order system, stable or unstable depending on the slope m_i.

3.4.1. Gain Scheduling

As previously mentioned, the gain scheduling will depend on vehicle speed and by that it is meant that the vehicle speed will scale the gain of the controller. At lower speeds the dynamics of the whole system start to oscillate and to compensate for this behavior the gain will be scaled by vehicle speed to lower value. Gain that the vehicle speed is scaling is equal to 0,045 and the vehicle speed entering the gain scheduling is expressed in m/s. The output of this gain scheduling algorithm is limited by upper limit of 1 and lower limit of 0,25 which is shown in Figure 16. Dividing the upper limit with the gain equals to 22,22 which is the maximum speed that is not affected by the gain scheduling, but if the vehicle speed value is lower than 22,22 m/s, gain will be scaled by the vehicle speed.

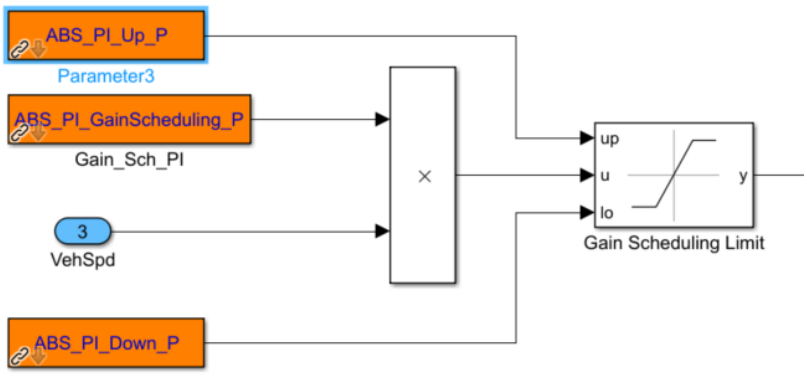

Figure 16. Vehicle speed gain scheduling

3.4.2. Anti-Windup compensator

Electromechanical brakes used in this simulation studies have a limit of braking torque at 5-6 kNm, so this characteristic should be limited. In this thesis maximum braking torque of

a single brake is set to 3 kNm, as it has been found that this amount of braking torque is enough to lock wheels.

When using controllers with integrators and without using special measures, integrator could windup over the physical limit of an actuator. Therefore, the integrator would have an output that the actuator couldn't perform. This problem is solved with an anti-windup compensator. There are many versions of the anti-windup compensators, and the version in Figure 17 is used.

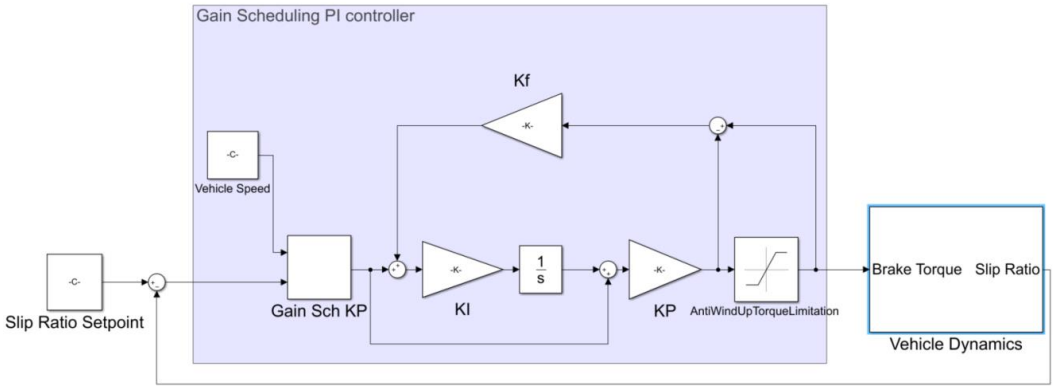

Figure 17. Gain Scheduling controller with anti-windup compensator

The compensator is only active when controller gives an output that is greater than the physical limit. The difference between the limit and the controller output is factored and fed back into the controller. The factor K_f has great effect on controller output value settling. Greater the factor value, shorter the settling time is, but oscillations and great overshooting can be experienced, so this factor should be calibrated until wanted behavior is achieved.

Proportional gains and integrator gains have been determined heuristically with trial-and-error-method. Used parameters are shown in the following Table 2.

Table 2. Gain Scheduling PI controller parameters

K_p	K_I	K_f
12000	3	0,05

3.5. Sliding mode control

Sliding mode control (SMC) is a nonlinear control method that alters the dynamics of a nonlinear system by application of a discontinuous control signal that forces the system to slide along a cross-section of the system's normal behavior. Sliding mode control is capable of handling system nonlinearities and has robust characteristics. By robust, it is meant that the

design of controller considers modeling uncertainties in the form of parameter uncertainties. Model imprecision may come from actual uncertainty, about the plant, or from the purposeful choice of a simplified representation of the system's dynamics. The typical structure of a sliding mode controller is composed of a nominal part, like a feedback linearizing or inverse control law, and of additional terms aimed at dealing with model uncertainty [13].

3.5.1. Sliding mode controller

In wheel slip control systems, application of sliding mode control is coupled with *brake-by-wire* systems because it exploits the maximum out of the electrical interface of the brakes [14]. Also, one of the reasons of using this control approach is because wheel slip dynamics has nonlinear characteristics. The control objective is to drive the wheel slip to target wheel slip, and controller input in this case is the braking torque. Equation (11) is used for this control law and it reads as:

$$\dot{\lambda} = \frac{1}{v_x}\left[\frac{r^2}{J}F_x + \frac{1}{m}(1+\lambda)F_x - \frac{r}{J}T_b\right] \tag{18}$$

The first step in designing a sliding mode controller is to define the so-called "*sliding surface"* s, and in this case, it can be defined as the error between the current slip and target slip. This conclusion reads [14]:

$$s = \lambda - \lambda_{ref} \tag{19}$$

As before mentioned the typical structure of a sliding mode controller is consisted of a nominal part and terms that are aimed at dealing with model uncertainty, so the following expression is defined as:

$$u = u_{eq} - k \cdot sign(s) \tag{20}$$

Equivalent system input u_{eq} corresponds to an inversion of the system dynamics, and parameter k or the control gain as it is called, covers model uncertainties and perturbations by depending on the sign of the function s, which in aftermath forces the state trajectory back onto sliding surface. Switching of the function remains until the following condition is met:

$$\dot{s} = \dot{\lambda} = 0 \tag{21}$$

Equivalent system input u_{eq} finally can be obtained when the previous condition is met. Combining Equation (18), (20) and (21) at the end gives:

$$u_{eq} = \left[r + \frac{J}{r \cdot m^*}(1+\lambda) \right] \hat{F}_x \quad \textbf{(22)}$$

Where $\hat{F}_x$ represents the estimated longitudinal tire force, and m^* represents the mass of vehicle upon the braked wheel. The control gain k, should be designed such that the control performance is robust to the estimation errors in longitudinal tire force. The control gain is determined from the following sliding condition [13]:

$$\frac{1}{2}\frac{d}{dt}s^2 \le -\eta|s| \quad \textbf{(23)}$$

Substituting Equation (21) into (23) gives the following condition

$$s\dot{\lambda} \le -\eta|s| \quad \textbf{(24)}$$

This condition can also be written as:

$$s\left\{ \frac{1}{v_x}\left[\frac{r^2}{J}F_x + \frac{1}{m}(1+\lambda)F_x \right] - \frac{r}{v_x J}u \right\} \le -\eta|s| \quad \textbf{(25)}$$

If control law from Equation (20) is used, the relation reads:

$$s\left\{ \frac{1}{v_x}\left[\frac{r^2}{J} + \frac{1}{m}(1+\lambda) \right]\left(F_x - \hat{F}_x\right) + \frac{r}{v_x J}k \cdot sign(s) \right\} \le -\eta|s| \quad \textbf{(26)}$$

Control gain k can be written as [14]:

$$k = -v_x \cdot \frac{J}{r}(N+\eta) \quad \textbf{(27)}$$

The scalar expression $(N+\eta)$ must be large enough to avoid any model uncertainties through parameter variations and simplifications in the model as well as the estimation errors of the longitudinal tire force must be considered. Also $s \cdot sign(s) = |s|$ can be considered for simplification. With all that said Equation (26) reads:

$$s \cdot \frac{1}{v_x}\left[\frac{r^2}{J} + \frac{1}{m}(1+\lambda) \right]\left(F_x - \hat{F}_x\right) + (N+\eta)|s| \le -\eta|s| \quad \textbf{(28)}$$

$$s \cdot \frac{1}{v_x}\left[\frac{r^2}{J} + \frac{1}{m}(1+\lambda) \right]\left(F_x - \hat{F}_x\right) \le N|s| \quad \textbf{(29)}$$

The task now is to find a suitable parameter N, by defining uncertainty of the longitudinal tire force that is limited by a constant:

$$\left|F_x - \hat{F}_x\right| \le B \quad \textbf{(30)}$$

$$N \geq \frac{1}{v_x}\left[\frac{r^2}{J}+\frac{1}{m^*}(1+\lambda)\right]\left|F_x-\hat{F}_x\right| \quad \textbf{(31)}$$

Combining Equations (30) and (31), parameter N reads as:

$$N \geq \frac{1}{v_x}\left[\frac{r^2}{J}+\frac{1}{m^*}(1+\lambda)\right]B \quad \textbf{(32)}$$

Finally, controller gain is written as:

$$k=-\left[r+\frac{J}{r\cdot m^*}(1+\lambda)\right]B-v_x\cdot\frac{J}{r}\eta \quad \textbf{(33)}$$

Substituting Equations (22) and (33) and into (20) results in sliding mode control law:

$$u=\left[r+\frac{J}{r\cdot m^*}(1+\lambda)\right]\hat{F}_x+\left\{\left[r+\frac{J}{r\cdot m^*}(1+\lambda)\right]B+v_x\cdot\frac{J}{r}\eta\right\}sign(s) \quad \textbf{(34)}$$

Parameters B and η are estimated through simulation and trial-and-error method and are chosen to avoid as much chattering as possible. They are shown in Table 3.

Table 3. Sliding Mode Control parameters

Sliding Mode Control parameters	
B	250
η	2

3.5.2. Chattering

Rattling or „chattering "as it is known can be problematic for mechanical systems in many ways. This phenomenon can excite vibrations in the drivetrain, which is ultimately an undesirably high-level strain on the actuator and the drivetrain itself. Chattering must therefore be avoided as much as possible or at least greatly reduced, so that the disadvantages outlined do not even occur.

In this thesis the following approach is used. The hard-switching sign function is replaced by a linear function within a boundary layer of certain width. This expressed mathematically reads as:

$$\text{sat}\left(\frac{s}{\phi}\right) = \begin{cases} +1 \text{ when } s>0 \\ \frac{s}{\phi} \text{ when } |s|\leq\phi \\ -1 \text{ when } s<0 \end{cases} \quad \textbf{(35)}$$

This boundary layer continues to have an attractive effect on the system trajectory. The system trajectory does not have to run exactly into the sliding state but may be within the boundary layer without switching. This worsens the controller accuracy. For use as a slip regulator, this loss of accuracy is still acceptable because the location of the optimal slip is not known beforehand and is therefore control accuracy does not need to be primary target.

3.6. Longitudinal tire force observers

In many control engineering and signal processing tasks, use of parameter observers is frequent. Using mathematical models of the observed system and correction calculation which compares the estimation and the measurement of the parameter, we the said parameter can't be measured directly. For before explained sliding mode controller good functionality, precise knowledge of longitudinal tire force is necessary. For this purpose, two observer approaches have been built up and compared against each other. First approach is the sliding mode observer that is based on a simple switching law. The second approach is using a Kalman Filter with a second order system model where the measurement is the angular velocity of a wheel and the observed states are also wheel angular velocity and longitudinal tire force.

3.6.1. Sliding mode observer

In [15] a simple, yet effective sliding mode observer is proposed which is based on basic wheel dynamics. Equation (7) can be used:

$$J \cdot \dot{\omega} = r \cdot F_x - T_b + T_d, \tag{36}$$

where T_d is an addition to the mentioned equation and it represents driving torque of the wheel. Output of the observer is an estimate of wheel angular velocity $\hat{\omega}$. Instead of the friction force, parameter V is introduced, so Equation (36) now reads [15]:

$$J \cdot \dot{\hat{\omega}} = r \cdot V - T_b + T_d, \tag{37}$$

where V is defined as [15]:

$$V = -M \cdot \mathrm{sgn}(\bar{\omega}), \tag{38}$$

where $\bar{\omega} = \omega - \hat{\omega}$ is a tracking error of the angular velocity and $M > 0$ is a large constant. The following condition should apply for correct working sliding mode observer [15]:

$$M > \max\{|F_x|\}. \tag{39}$$

After looking at the tire model used in this study, it has been seen that the maximum longitudinal force that can be exerted on this tire is around 9900 N. For that reason, M is equal to 10000. With this condition it is guaranteed that the wheel angular velocity estimation will slide, no

matter how great the friction force on a tire is. This condition also has some drawbacks. Observers goal is that the tracking error of the angular velocity tends towards 0. Consequences are oscillations at high frequencies, so before the longitudinal force is fed into the sliding mode controller, signal should pass through a low pass filter. This is done with the help of a first order low pass filter.

Equation of the filter reads as [15]:

$$W_f(s) = \frac{1}{T_f \cdot s + 1}, \tag{40}$$

Where time constant T_f is chosen to suppress the high frequency of the oscillations, but not to disturb the observer functionality. With trial and error method T_f is chosen and it is equal to 0.08 s.

Finally, the equation for estimated longitudinal force reads as:

$$\hat{F}_x(s) = W_f(s) \cdot V\,. \tag{41}$$

3.6.2. Kalman filter

Longitudinal tire force can also be estimated by using a Kalman filter. Kalman filtering is an algorithm that uses a series of measurements observed over time, containing statistical noise and other inaccuracies, and produces estimates of unknown variables that tend to be more accurate than those based on a single measurement alone. In this method uncertainties in modeling, noisy measurements and disturbances are considered. For the estimation of the tire longitudinal force, linear time invariant state space model is used, and electromechanical brake torque is used as well.

Kalman filter is widely used as an unknown input estimator. It models the evolution of unknown input signals as a random walk. Before the Kalman filter is discussed, Equation (7) is derived by using Euler's method. [16].

$$\omega(k+1) = \omega(k) + h\dot{\omega}(k) \tag{42}$$

Wheel angular velocity is derived and then inserted in Equation (42):

$$\omega(k+1) = -h\frac{r}{J}F_x + h\frac{T_b}{J} + \omega(k) \tag{43}$$

Where h is the sampling time and k is the number of steps in Kalman filter estimation. Data acquisition rate is around 100 Hz, so h is equal to 10 ms. Then the state-space representation of wheel dynamic model for the Kalman filter is [16]:

$$\begin{aligned} F_x(k+1) &= F_x(k) + w_1(k) \\ \omega(k+1) &= \omega(k) - h\frac{r}{J}F_x + h\frac{\tau(k)}{J} + w_2(k) \\ y(k) &= \omega(k) + v(k) \end{aligned} \quad \textbf{(44)}$$

where w_1 is the random walk signal that causes the update of tire force F_x, w_2 is the unmeasured process disturbance acting on the wheels and v_k is the measurement noise from the wheel speed sensor, which is treated as the measured input signal here. The system input $\tau(k)$ is defined as the sum of drive torque and brake torque acting on the wheel. Brake torque that is a part of the systems input also includes the actuator brake dynamics. Finally, system input is defined as:

$$\tau(k) = T_d(k) + T_b(k) \quad \textbf{(45)}$$

If the state vector is defined as:

$$x(k) = \left[F_x(k)\ \ \omega(k)\right]^T \quad \textbf{(46)}$$

The above-mentioned wheel dynamics model can be rewritten as a standard state-space form:

$$\begin{aligned} x(k+1) &= Ax(k) + B\tau(k) + w(k) \\ y(k) &= Cx(k) + v(k) \end{aligned} \quad \textbf{(47)}$$

Matrices *A*, *B* and *C* are defined as follows:

$$A = \begin{pmatrix} 1 & 0 \\ -h\frac{r}{J} & 1 \end{pmatrix} \quad B = \begin{pmatrix} 0 \\ h\frac{1}{J} \end{pmatrix} \quad \textbf{(48)}$$
$$C = (0\ 1)$$

The covariance matrices $Q(k)$ of the process noise and $R(k)$ of the measurement noise read as:

$$\begin{aligned} Q(k) &= E\begin{pmatrix} w_1^2(k) & w_1(k)\cdot w_2(k) \\ w_2(k)\cdot w_1(k) & w_2^2(k) \end{pmatrix} \\ R(k) &= E(v^2(k)) \end{aligned} \quad \textbf{(49)}$$

where *E* is the eigenmatrix. It is usually assumed that the noise vectors are uncorrelated among themselves, which is why the covariance matrices are defined as diagonal matrices. The objective of the Kalman filter is to optimally estimate the unknown input signal $F_x(k)$ in terms of the minimum-variance criterion. The Kalman filter equations for each step are summarized in following Equation (50):

$$\begin{aligned} P_k^- &= AP_{k-1}^+A^T + Q_{k-1} \\ K_k &= P_k^-C^T(CP_k^-C^T + R)^{-1} \\ \hat{x}_k^- &= A\hat{x}_{k-1}^+ + Bu_{k-1} \\ \hat{x}_k^+ &= \hat{x}_k^- + K_k(y_k - C\hat{x}_k^-) \\ P_k^+ &= (1 - K_kC)P_k^- \end{aligned} \quad \textbf{(50)}$$

where:

- $\hat{x}_k^-$ a-priori state vector update,
- $\hat{x}_k^+$ a-posteriori state vector update,
- P_k^+ a-priori error covariance matrix updates,
- P_k^- a-posteriori error covariance matrix updates,
- K_k Kalman gain matrix

The covariance matrices Q and R must be known beforehand. Since the values of said covariance matrices are usually not known, they can be used as tuning parameters of the estimate value convergence. The greater the value of the covariance matrix, the greater the noise, which represents more uncertainty of estimated value. The wheel angular velocity is measured precisely, and the measurement noise is present only due to the quantization noise of the given digital measured signal and therefore it is neglected. Q and R have been defined with trial and error method:

$$Q = \begin{bmatrix} 10^8 & 0 \\ 0 & 10^{-2} \end{bmatrix}$$
$$R = 10 \qquad \textbf{(51)}$$

3.6.3. Simulation analysis of proposed observer designs

As the longitudinal tire force observers and their principle of operation has been explained, it will be determined, which performs better. For that reason, simulation analysis of the said observers has been conducted in MATLAB/Simulink® software package. As the robustness of the observers needs to be checked, they have been tested on a μ - *Step* brake maneuver, where the friction coefficient changes two times during braking. As these longitudinal tire force observers have been built up for *Sliding Mode Control*, it will be used for this analysis. Because of friction coefficient change, estimation of longitudinal force will be demanding for the observers, as the transient behavior can be expected.

In Figure 18, estimation result of sliding mode observer is presented. Blue line on the graph marks the estimated value of the longitudinal tire force, whereas the orange presents the real value of the said force. Generally, estimation of the longitudinal force resembles the real value, but on several occasions' observer response is slow. This can be seen at the start of the maneuver when the vehicle is starting from a standing point. Same behavior is exhibited when

the accelerator pedal position is changed. Also, when the brake pedal is pressed it takes about 0,2 s to reach the real value, and the oscillations at the end of the maneuver, between 13 and 14,4 s are estimated roughly.

In Figure 19, Kalman filter estimation result is presented. From a brief look at the results the Kalman Filter estimation is more precise, and it reacts faster than the sliding mode observer. Especially, the oscillations between 13 and 14,4 s are captured to a better extent. In Figures 19 and 20 the error between the real and estimated values is shown. Locally sliding mode observer has smaller value errors, but they do not settle quickly as it is the case with the Kalman filter. With Kalman filter at 10,7 s huge error is visible, but it settles in under 0,01 s.

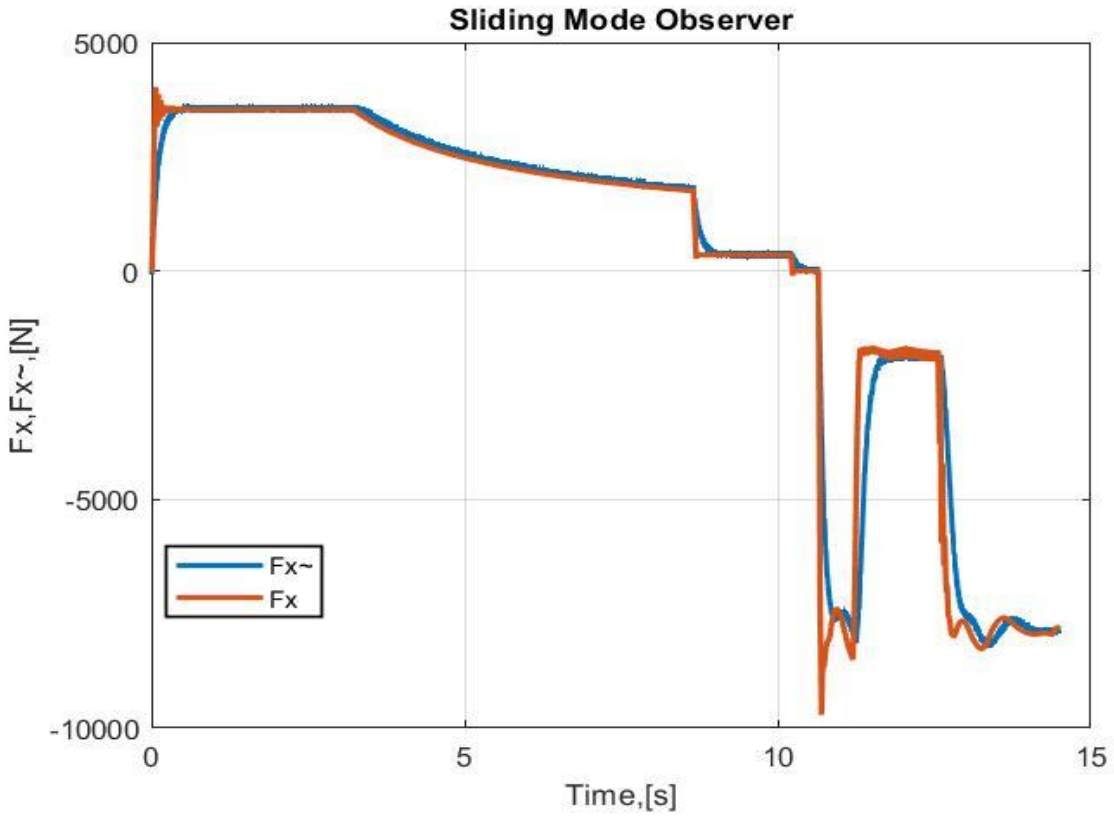

Figure 18. Sliding mode observer estimation

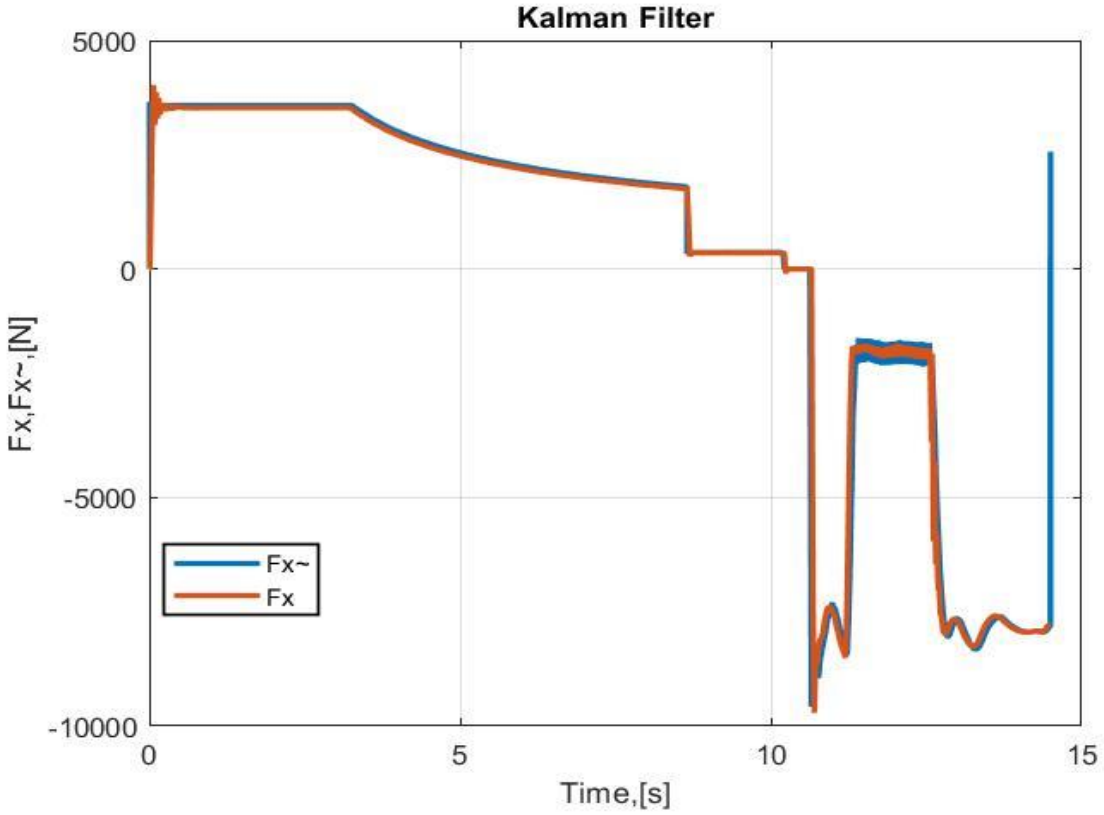

Figure 19. Kalman filter estimation

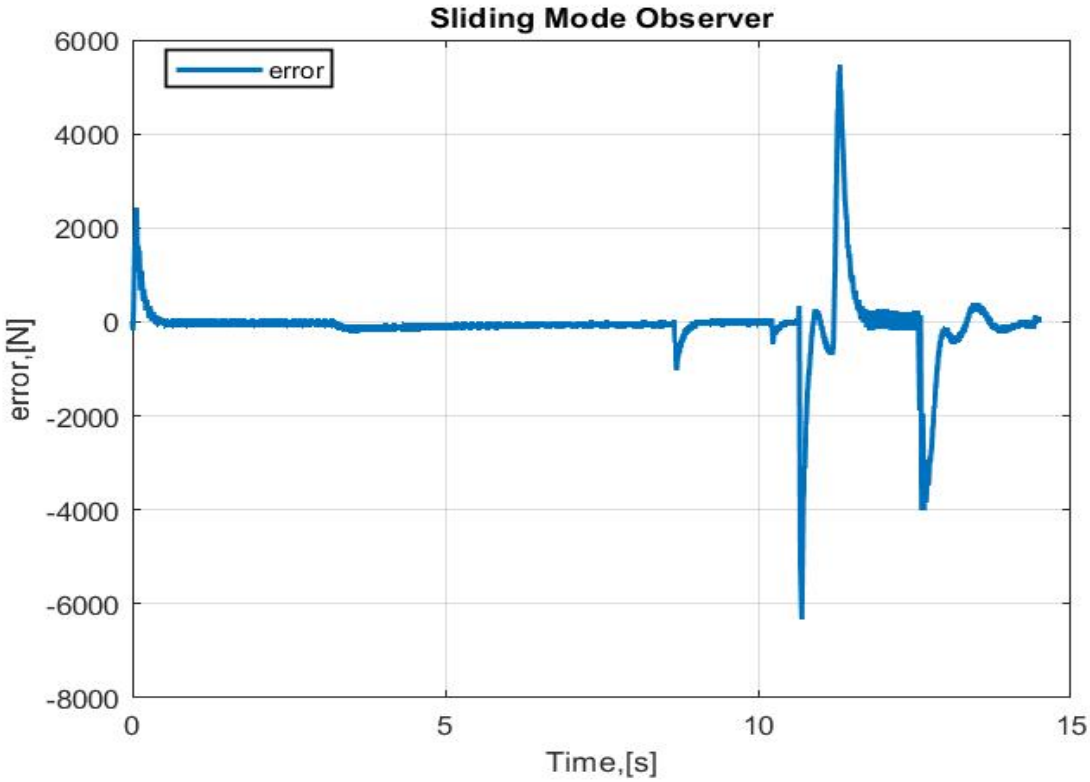

Figure 20. Sliding Mode Observer error

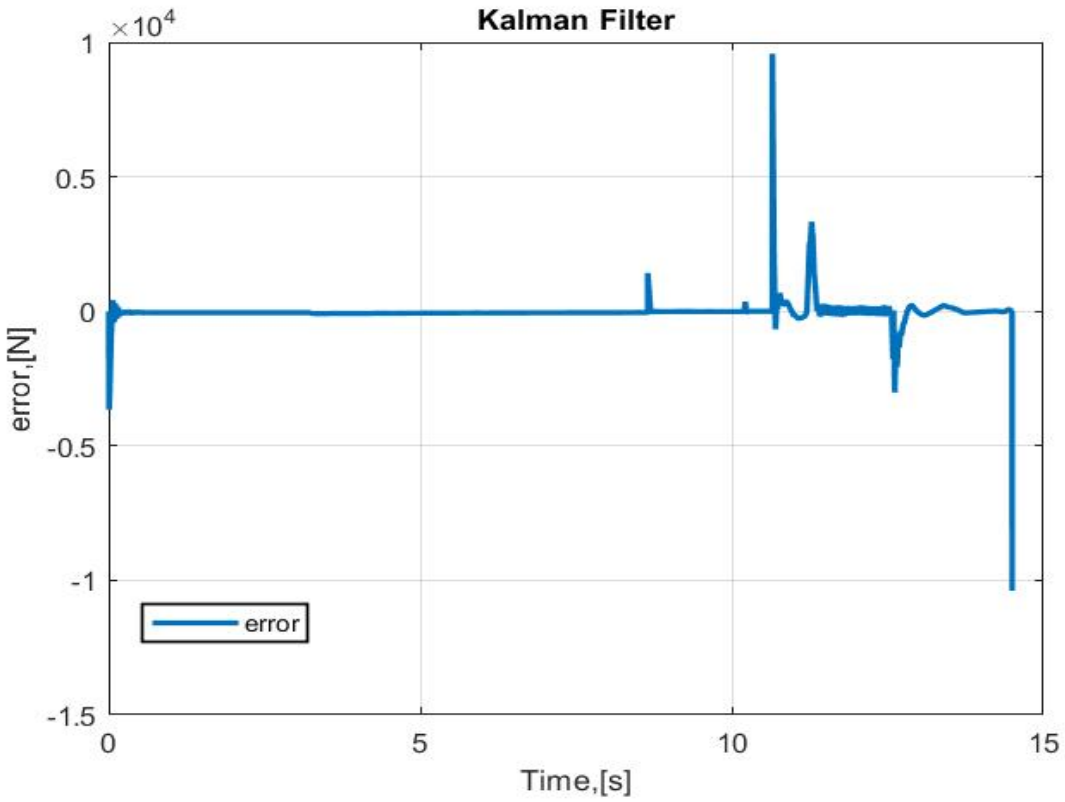

Figure 21. Kalman Filter error

The main reason behind the slow response of the Sliding mode observer is the noise filter that is implemented to reduce the effect of chattering. The smaller the value of the filters time constant, faster the response will be, but the downside is that the output of the observer will be chattery and this behavior could cause unstable operation of the controller.

Calculated performance indication can be done by integrating the estimation error from start to the end of the maneuver. But for this purpose, the section from t_1=10,7 s and t_2=14,7 s, whilst braking occurred, can be examined independently since the scope of this work only considers braking performance at test maneuvers. After defining how the performance will be graded, mathematical equation needs to be defined. The following Equation (52) reads:

$$E_{F_x} = \int_{t_1}^{t_2} \left| \hat{F}_x(t) - F_x(t) \right| dt \tag{52}$$

After calculating the error, the results are shown in Table 4.

Table 4. Observer errors

Error	Sliding Mode	Kalman Filter	Time period
E_{F_x}	4406,7	2126,3	t_1=0; t_2=10,7
$E_{F_x,rel}$	207,2%	100%	
E_{F_x}	3408,5	1404,5	t_1=10,7; t_2=14,4
$E_{F_x,rel}$	242,7%	100%	

Results are showing that Kalman filter estimation error is smaller by 2 times in comparison with the Sliding mode observer. As previously assumed, most of the estimation error comes from braking period between t_1=10.7 s and t_2=14.7 s. Sliding mode observer design is simpler than the Kalman filter design, and it can be assumed that the vehicles ECU would benefit from this, because it is easier to process a simpler design, but in terms of simulation analysis Kalman filter has better performance.

4. CO-SIMULATION ENVIROMENT WITH AVL VSM™ AND MATLAB/SIMULINK®

Electromechanical brake dynamics and anti-lock braking controllers have been defined and for their part of simulation MATLAB/Simulink® software package will be used because of its simplicity and good overview of different parameters used in control laws, which in this case is highly useful. Vehicle dynamics also must be defined and for this part AVL VSM™ will be used.

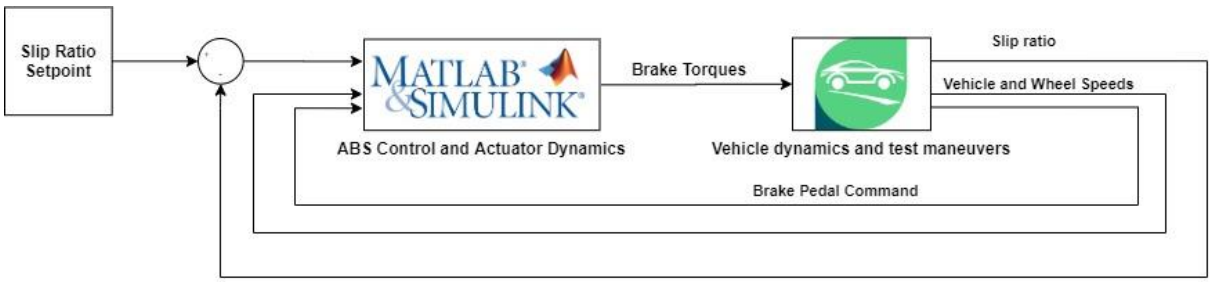

Figure 22. Co-simulation environment

Through AVL VSM™ interface parameters of the vehicle model can be defined quickly and besides that, test maneuvers can be defined as well. Test maneuvers in AVL VSM™ are defined with parameters like distance, surface grip, starting speed etc. Detailed definition of test maneuvers will be explained in chapter 5. When all necessary parameters for simulation analysis are defined in AVL VSM™, they can be exported to MATLAB workspace and then they can be coupled to anti-lock braking controller as it can be seen in Figure 22.

AVL VSM™ outputs of slip ratio, vehicle and wheel speeds are used by proposed ABS controller to calculate the braking torque to achieve the slip ratio that is set as a setpoint value. Brake pedal command from the AVL VSM™ driver acts as a limit to the controller output of braking torque. If there was not any limit on the braking torque output, the controller would try to brake the wheels to achieve the setpoint value of slip ratio, no matter what the demanded braking torque from the AVL VSM™ driver was.

4.1. Vehicle model

To complete the whole feedback loop, vehicle model needs to be defined. Vehicle used in this project is VW e-Golf which is shown in Figure 23. Originally this vehicle is equipped with hydraulic brakes both on front and rear axles, but in this study the front hydraulic brakes are going to be swapped with electromechanical brakes. Rear hydraulic brakes will remain on the vehicle, but for the purpose of this simulation studies they will not be used. Main reason

behind this is that the rear wheel speeds can be used as a reliable source for vehicle speed calculation, therefore complicated vehicle speed estimation filters do not have to be designed. This brake configuration layout will be used in simulation analysis where the proposed ABS controllers will be compared.

However, to have a comparable data to conventional ABS, all four wheels must be braked. For this case rear wheel speeds cannot be used for vehicle speed calculation. Vehicle speed used in this case will be taken from AVL VSM^{TM} calculation, but if these proposed ABS controllers will be implemented on a rear vehicle where all four wheels are braked, the above-mentioned vehicle speed estimation filter should be built up. For simulation purposes, a simple electric motor brake model will be built up, and two of these electric motor brakes will be connected to each rear wheel separately. They will be just used as a brake actuators, since the vehicle already has a drive electric motor connected to front wheels over a single-speed gearbox, and this drive electric motor connected to the front will not be used for braking.

To conclude, two brake layout configurations will be conducted to simulation analysis. First one will just have the two front EMB brakes. The second layout will also have two EMB brakes mounted at the front wheels, but also two electric motor brakes will be directly coupled to rear wheels, and act as brake actuators. Logic of braking distribution between the EMBs and electric motors will be explained later. Main vehicle parameters used in this simulation analysis are shown in Table 5.

Table 5. Vehicle model parameters

Parameter	Value
Vehicle mass, m	1628 kg
Tire radius, r	0,32 m
Wheel and motor inertia, J	3 kgm^2

Figure 23. VW e-Golf 2017[17]

4.2. Electric motor brake actuator

In scope of this thesis, the focus was put on braking with electromechanical brakes and tuning the controller to EMB dynamics. However, because of EMBs electrical interface, built up controllers can be coupled to the electric motor brake. Electric motors have an advantage over EMBs in a view of faster torque response, which can be of great importance in emergency braking situations. However, there are some downsides to the braking with electric motors. Electric motors cannot output a lot of braking torque in comparison with the electromechanical brakes and sometimes they cannot match the demanded braking torque. This problem is solved with gearboxes which are increasing the motors output torque by a fixed transmission ratio, but there is limit to the transmission ratio in terms of gearbox mass and overall size.

Used electric motor characteristics for this simulation analysis are shown in Figure 24.

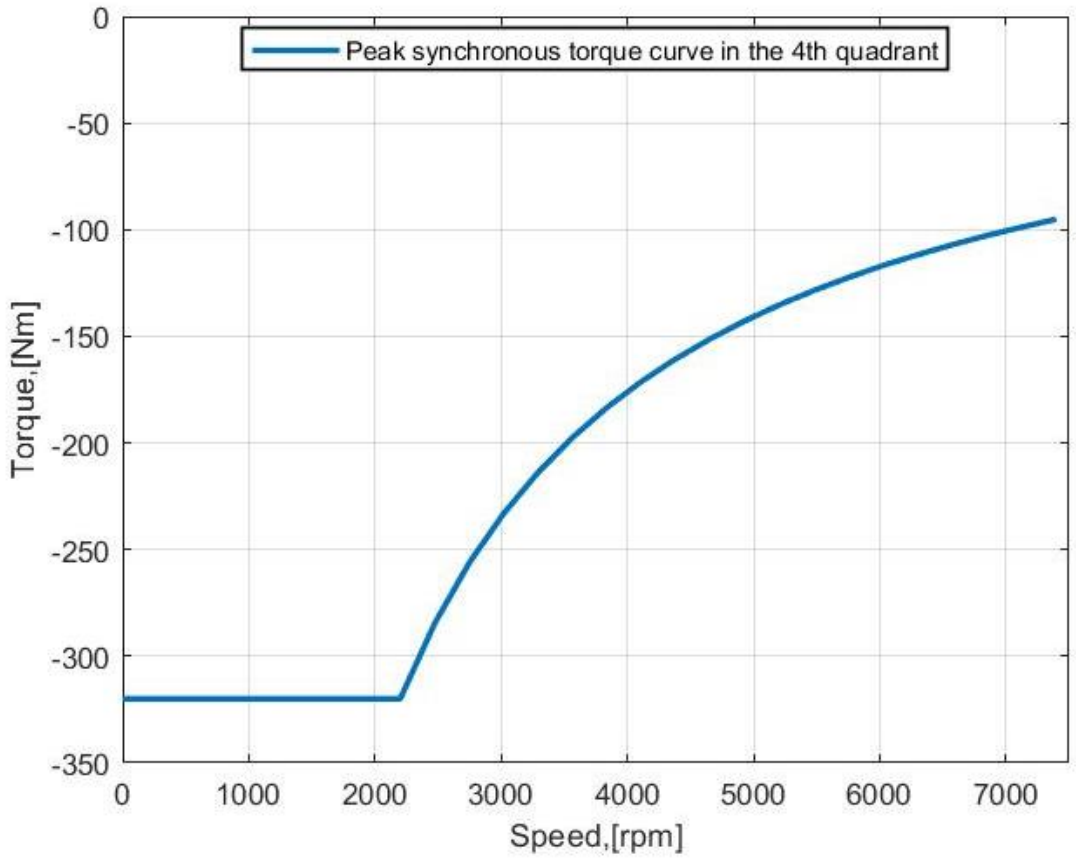

Figure 24. Electric motor characteristics

Relation between torque demand and torque output of the electric motor has been modeled as a simple delay, and in further work the model can be expanded by using mathematical equations and other physical laws. Delay is modeled as a first order transfer function where the time constant is equal to 0,015 s.

4.3. Brake torque distribution

In order to provide an appropriate motor brake torque for a given driving condition, a control algorithm is required to determine the allocation of the electric motor brake and electromechanical brake corresponding to the driver braking demand. If the required braking motor torque is smaller than the maximum possible braking torque, then braking distribution is set to fixed value of 65:35, where the 65% of braking torque is allocated to the front wheels and the 35% is allocated to rear wheels. When demanded braking torque is larger than the maximum possible braking torque, electromechanical friction brake has to compensate the missing torque. With all that said, simple decision algorithm can be presented on Figure 25.

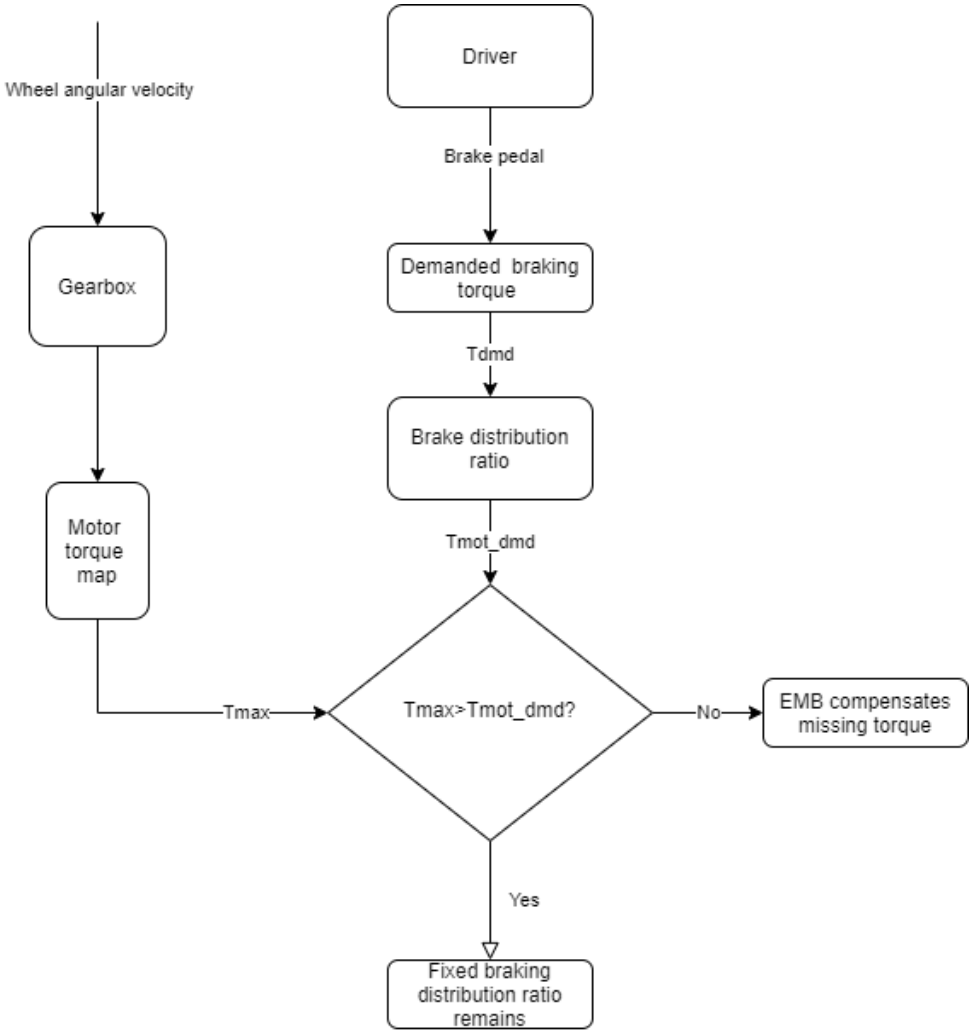

Figure 25. Braking torque allocation flowchart

4.4. Downsampling

Default AVL VSM™ integration step is rated at 2000 Hz, but as already mentioned, automotive ECUs are rated at about 100 Hz, so to be sure that ABS controllers are robust enough to perform on smaller calculation rates, wheel speed sample rate is downsampled by 20 times as shown in Figure 26.

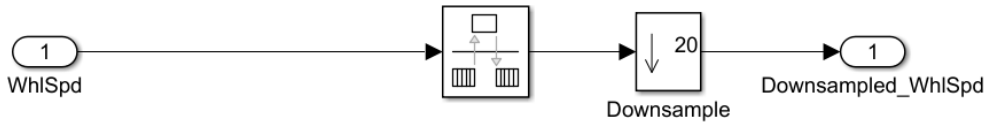

Figure 26. Downsampling

4.5. Torque difference limiter

Besides the controllers, other auxiliary functions have been implemented to ensure good functioning of the system in whole. Often, the road conditions can vary, especially when the road is damp, so the road surface grip can be different from patch to patch. Also, sometimes drivers find themselves in emergency braking situations, when one side of the vehicle is placed on the asphalt, and the other one is placed on grass next to the road. The slip ratio value in this thesis is the setpoint value, and it's fixed no matter what the road conditions are. As it can be seen from Figure 13, on surfaces with low friction coefficients, same slip value can be achieved as on surfaces with high friction coefficients, with less braking torque. If the controller works as it should, whilst braking in the mentioned situations, higher torque will be applied on the wheel with more surface grip than on the wheel with less surface grip. This will cause a yaw moment around the center of gravity of a vehicle, which in aftermath turns the vehicle under braking and it makes it unstable. To overcome this, a torque difference limiter shown in Figure 27 is implemented.

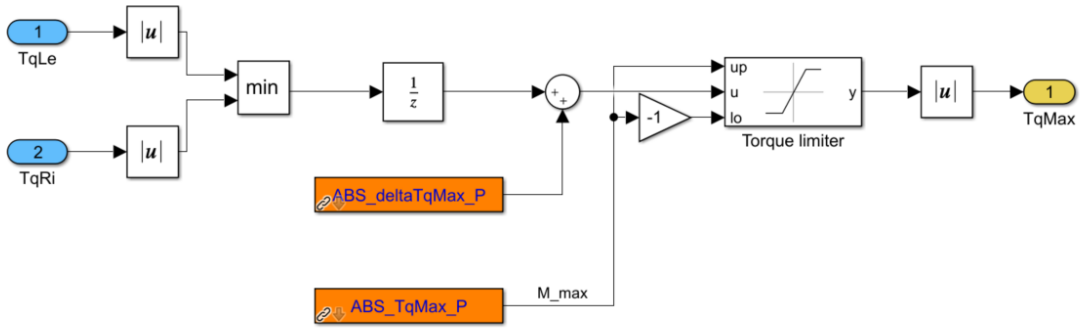

Figure 27. Torque difference limiter

Absolute braking torque of left and right wheels are inserted into the limiter, and the smaller value of the two is chosen. Fixed value of maximum torque difference is added to the smaller braking torque. This value is then fed out of the model, and it acts as a torque limiter to the higher braking torque. Also, unit delay is implemented, so the limiting does not occur to fast, as the driver will have more reaction time. With this limiter there can be some downsides. If the fixed difference is set to low, there is a possibility that the deceleration of the vehicle will be small. On the other hand, if the value is set high, yaw motion can occur during braking, so the value should be set accordingly, to get the wanted behavior.

5. TEST MANEUVERS AND SIMULATION RESULTS

After defining the anti-lock brake controllers and vehicle parameters, maneuvers that are typical for ABS and brake systems testing will be conducted, in order to assess the performance of the controller itself and its robustness against changing road conditions, white measurement noise, wheel loads etc. Six following maneuvers will be conducted: *μ - High* and *μ - Low*, *μ - High to μ - Low* and vice versa, *μ - Step* and *μ - Split*. Two road friction coefficients are going to be used throughout the said maneuvers, one that corresponds dry asphalt ($\mu_{high} = 1$), and the second one that corresponds to hard packed snow road ($\mu_{low} = 0,3$). The vehicle speed at the start of the all maneuvers equals to 100 km/h, except the *μ* -Low maneuver where the starting speed is equal to 60 km/h. Slip ratio is the regulated parameter and the setpoint value of slip ratio equals to -0,09, because at this value, the tire models that are used in this simulation analysis have the greatest friction coefficient in longitudinal direction.

μ - High is a simple maneuver where the vehicle is braking on dry asphalt ($\mu_{high} = 1$) from 100 km/h to full stop. *μ - Low* maneuver is a similar one, where the vehicle is braking from 60 km/h to full stop, but on a hard-packed snow road ($\mu_{low} = 0,3$). *μ - High to μ - Low* maneuver also starts with 100 km/h, but during braking, the friction changes from previously declared high to low friction coefficient. *μ - Low to μ - High* works on same principle, but the vehicle first starts braking on low friction coefficient surface. *μ - Step* is a braking maneuver where the vehicle starts braking on high friction surface, but during braking, the friction coefficient changes twice, firstly from high to low and then from low to high friction coefficient. And finally, *μ - Split* is a maneuver where the vehicle also starts braking on high friction surface, but during braking one side of the vehicle starts braking on low friction surface, and the other one is still braking on the high friction surface. Every mentioned maneuver is simulated with 100% braking torque demand. The described maneuvers are presented in Table 6 for more accessible overview.

Simulation step time of the co-simulation environment originally is equal to 0,5 ms, but as real-life situation wants to be replicated in simulation, fixed step time is upscaled to 10 ms, which is often calculation time of ABS control units or ECUs.

Table 6. Test maneuver descriptions

Test Maneuver	Test Maneuver Description	Start Speed / Grip level
μ - High	Braking from 100 km/h to 0 km/h on a *μ - High* surface	100 km/h / 100%
μ - Low	Braking from 60 km/h to 0 km/h on a *μ - Low* surface	60 km/h / 30%
μ - High to μ - Low	Braking from 100 km/h to 0 km/h on a *μ* changing surface from *High* to *Low*	100 km/h / 100% - 30%
μ - Low to μ - High	Braking from 100 km/h to 0 km/h on a *μ* changing surface from *Low* to *High*	100 km/h / 30%-100%
μ - Step	Braking from 100 km/h to 0 km/h on a *μ* changing surface from *High* to *Low* and again back to *High*	100 km/h / 100% - 30%-100%
μ - Split	Braking from 100 km/h to 0 km/h on a *μ* changing surface from *High* to *Low* just for one side of the vehicle, whilst the other is still on *μ - High* surface	100 km/h / 100% - 30%

5.1. Key performance indicators

As two controller performances are going to be assessed, measurable parameters must be defined to establish, which controller behaves better in comparison with the other controller based on the said parameters. These parameters are called key performance indicators or KPIs. Each set of KPIs will be defined for each maneuver specifically, in order to get a clear picture, which controller performs better given the circumstances. Following KPIs will give assessment of controller performance and vehicle dynamics stability:

- Brake Distance (BD) - The brake distance is defined as the velocity integral from the moment at which the brake pedal is first pressed (t_1) to that in which the vehicle speed equals the exit velocity of 0. The aim is to compare overall braking distance of both controllers

$$BD = \int_{t_1}^{t_2} v_{veh} dt \tag{53}$$

- Mean Deceleration (MD) - This is simply the mean longitudinal deceleration calculated in a time interval that goes from 90% to 5% of the vehicle speed at the beginning of the braking. The MD is specifically designed for assessment the vehicle deceleration performance throughout the entire ABS activation time [18].

$$MD = \left| \dot{\overline{v}}_x \right|_{0.05v}^{0.9v} \tag{54}$$

- Integral Pitch Variation (IPV) - Research has shown that the vehicle pitching motion affects the driver capabilities to estimate distances, it is therefore desirable for an ABS to be as smooth as possible in its control action. IPV is mostly relevant on high friction surfaces but it will be calculated for other maneuvers as well [18].

$$IPV = \int_{t_1}^{t_2} \left| \dot{\psi} \right| dt \tag{55}$$

- Integral Yaw Variation (YV) - On μ - *Split* maneuver, yaw angle variation can occur during braking on a different level surface grip. Possible yaw motion driver-in-loop will try to correct.

$$IYV = \int_{t_1}^{t_2} \left| \dot{\phi} \right| dt \tag{56}$$

- Slip Error (SE) – This is a simple KPI that will assess the controller performance in terms of following the given setpoint of slip ratio, from when the brake is pressed up to the point where the vehicle reaches full stop. Low frequency oscillations will not be considered, so a high pass filter is used.

$$SE = \int_{t_1}^{t_2} G(s)\left(\lambda_{ref} - \lambda\right)^2 dt \tag{57}$$

$$G(s) = \frac{s}{s + 20} \tag{58}$$

- Maximum Slip Error (SE) – This KPI is also oriented on controller performance, and it calculates the biggest deviation of slip ratio from setpoint value.

$$MSE = \left| \lambda_{ref} - \lambda \right| \tag{59}$$

5.2. Test maneuver results for the case of EMBs

After conducting previously specified test maneuvers, the behavior and performance of the *Gain Scheduling PI* and *Sliding Mode Control* controllers coupled with just electromechanical brakes mounted on the front wheels will be presented in following Figures.

5.2.1. μ - High

After simulating the *μ - High* maneuver, results for the *Gain Scheduling PI* control are presented in Figure 28 and results for the *Sliding Mode Control* are presented in Figure 29. From starting point of braking to slip value settling the behavior of both controllers isn't very different. Difference can be seen from settling point to the vehicles full stop. The *Gain Scheduling PI* controller has less slip error and it tracks the set value better than the *Sliding Mode Control* based ABS controller.

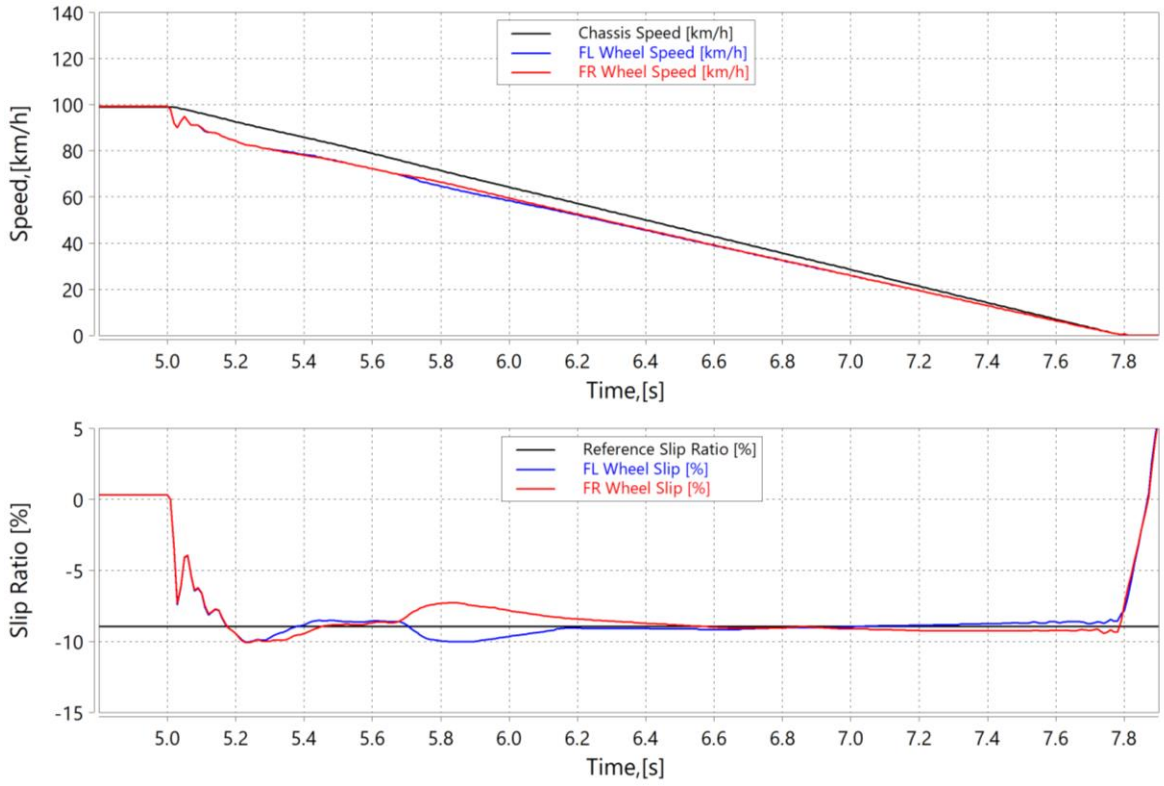

Figure 28. μ-High Gain PI Scheduling

From the standpoint of stability and driving comfort, *Gain Scheduling PI* controller is also showing better performance, as the yaw and pitch angles are changing less during braking as it is visible from Table 7. *Sliding Mode Control* based ABS controller, has a shorter stopping distance due to faster response of the controller itself. Mean deceleration value is smaller, but the period from braking start to slip value settling shows critical for this performance indicator.

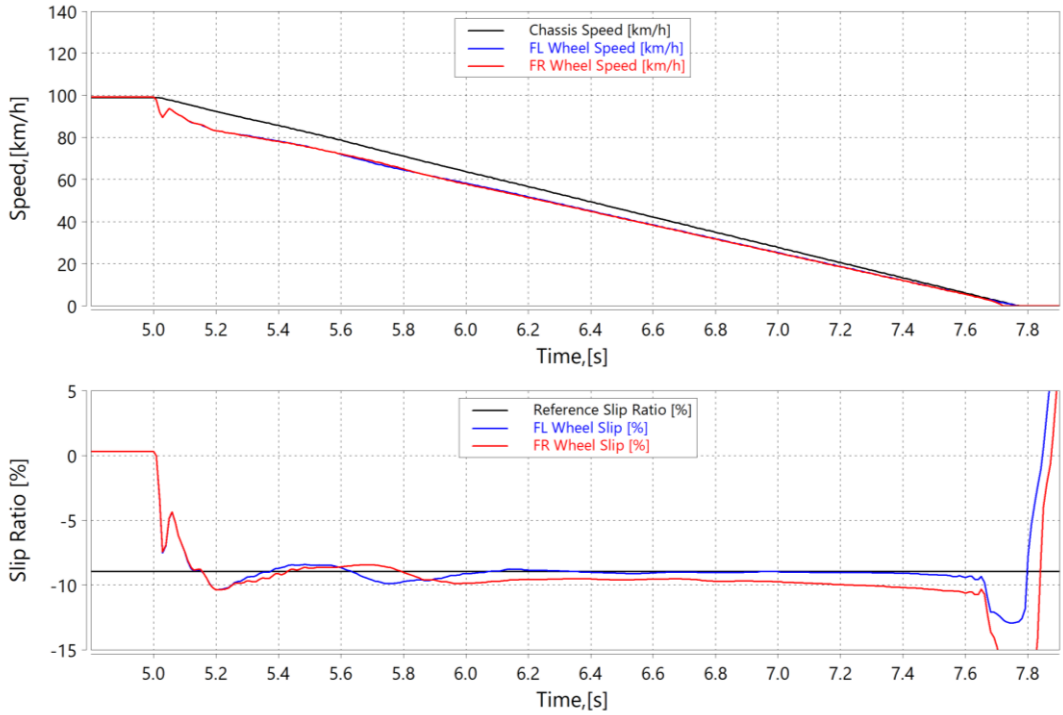

Figure 29. µ-High Sliding Mode Control

Table 7. µ-High KPI comparison

KPI \ ABS controller	Gain PI	SMC
BD [m]	38,75435163	38,38139828
IPV [deg]	7,990301272	9,257110493
IYV [deg]	15,04910039	16,79687302
MD [m/s^2]	9,87509781	9,857123197
MSE [-]	0,006726955	0,010330015
SE [-]	0,033378515	0,8992406

5.2.2. μ - Low

After conducting the *μ - Low* maneuver, some differences in performance can be seen if it is looked at the relative comparison of the proposed controllers. The *Gain Scheduling PI* controller shown in Figure 30 has a much bigger overshoot and oscillatory behavior at the start of the braking than the *Sliding Mode Controller* shown in Figure 31, but again after settling the first mentioned controller tracks the setpoint value with more precision than the SMC. The oscillations of *Gain Scheduling PI* controller could be avoided with another set of parameters that are suitable for low grip surfaces, but again that set of parameters would not perform good on high grip surfaces, so a potential for a scheduling variable in terms of friction coefficient can be considered for future work. SMC shows greater yaw motion of the vehicle due to faster and aggressive response on torque command, and the pitch motion is the same. Stopping distance is again shorter for the SMC controller, but the difference is negligible. KPIs are given in Table 8.

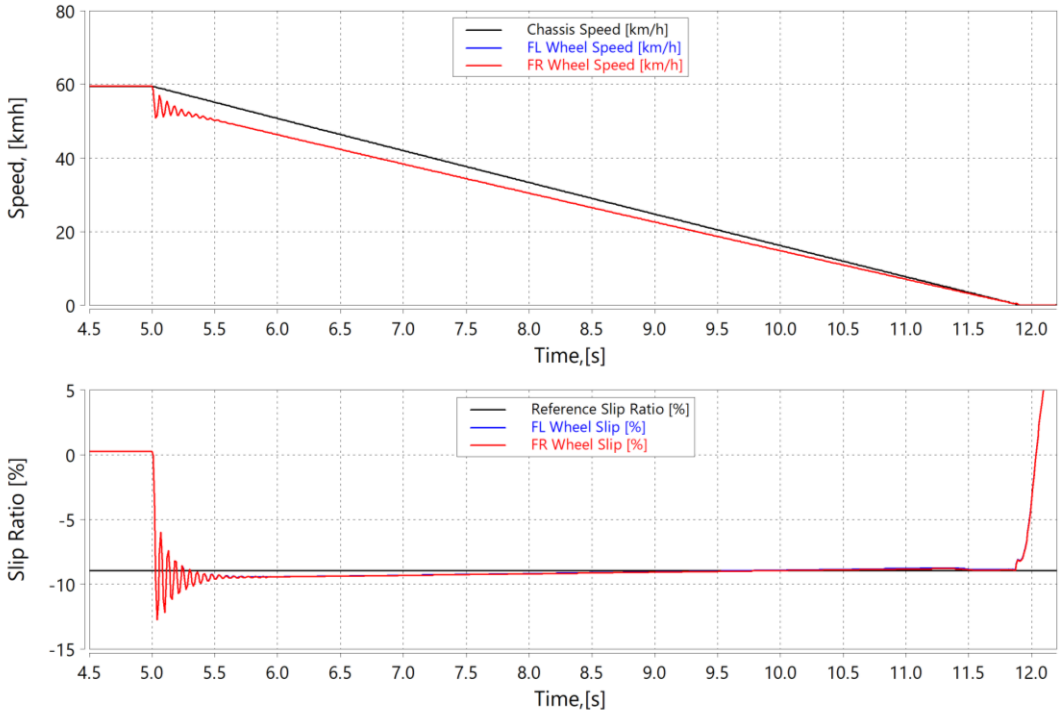

Figure 30. μ-Low Gain PI Scheduling

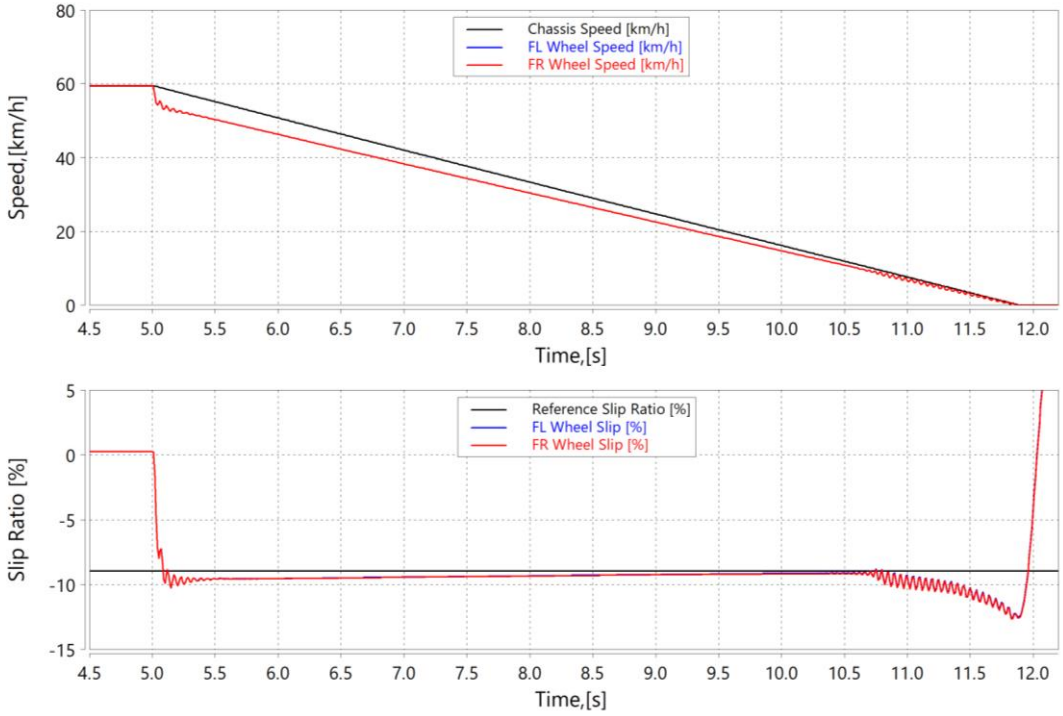

Figure 31. μ-Low Sliding Mode Control

Table 8. μ-Low KPI comparison

KPI \ ABS controller	Gain PI	SMC
BD [m]	56,5570701	56,33279537
IPV [deg]	0,45109836	0,420617801
IYV [deg]	2,980525211	3,650849031
MD [m/s^2]	2,38898448	2,389199772
MSE [-]	0,057007106	0,01358357
SE [-]	0,025810029	0,03145676

5.2.3. μ - High to μ - Low

μ - High to μ - Low maneuver has been conducted, and the switch from high friction surface to low friction surface is manifested in a small overshoot of slip value. Both controllers have similar behavior, but the SMC controller shown in Figure 34 has smaller overshoot and settles faster than *Gain Scheduling PI* controller shown in Figure 33. Again, similar relative performance is seen for both controllers regarding the vehicle stability and braking distances. Overshoot could be compensated with a faster EMB response or with a different set of proportional gains, integrator gains or tuning parameters that are more suitable for low surface grip conditions. Timestamp of friction coefficient change is shown in Figure 32 and KPIs are given in Table 9.

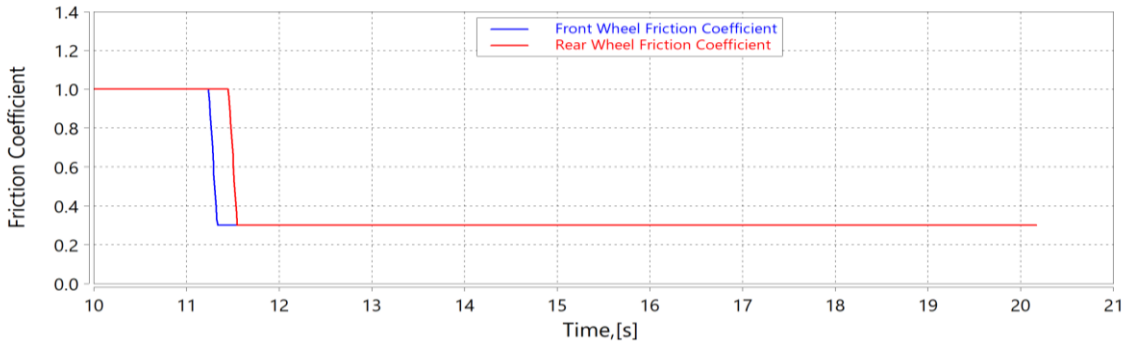

Figure 32. μ-High to μ-Low friction coefficient change

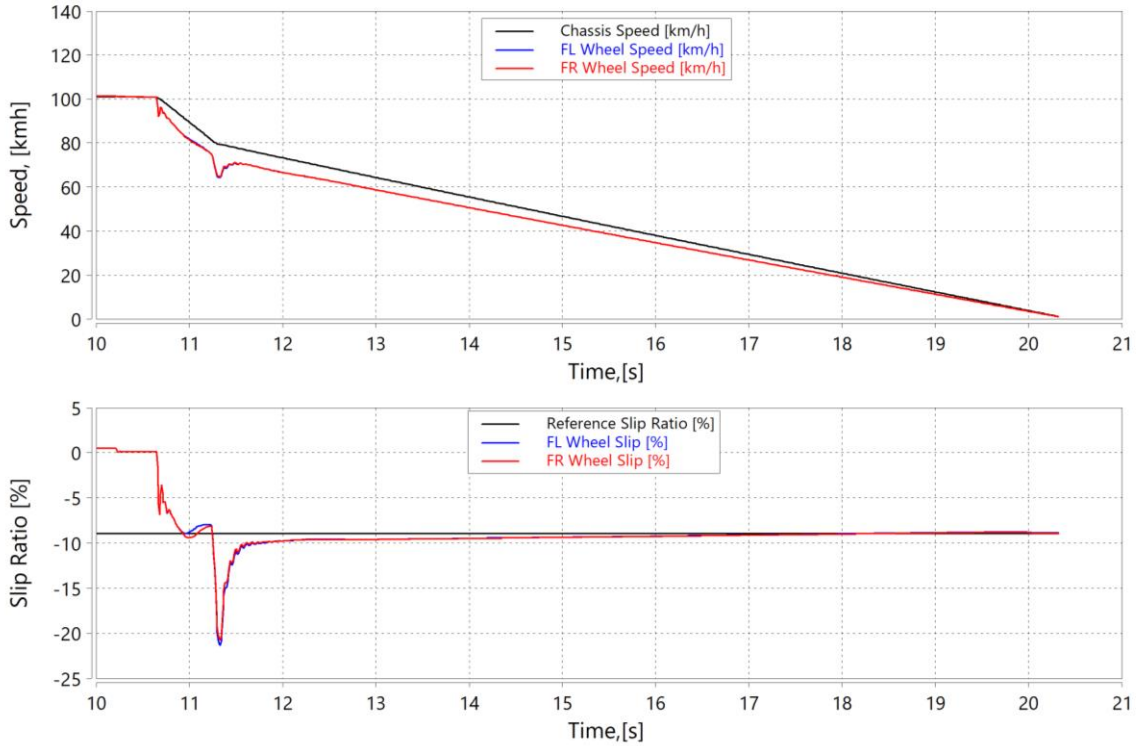

Figure 33. μ-High to μ-Low Gain Scheduling PI

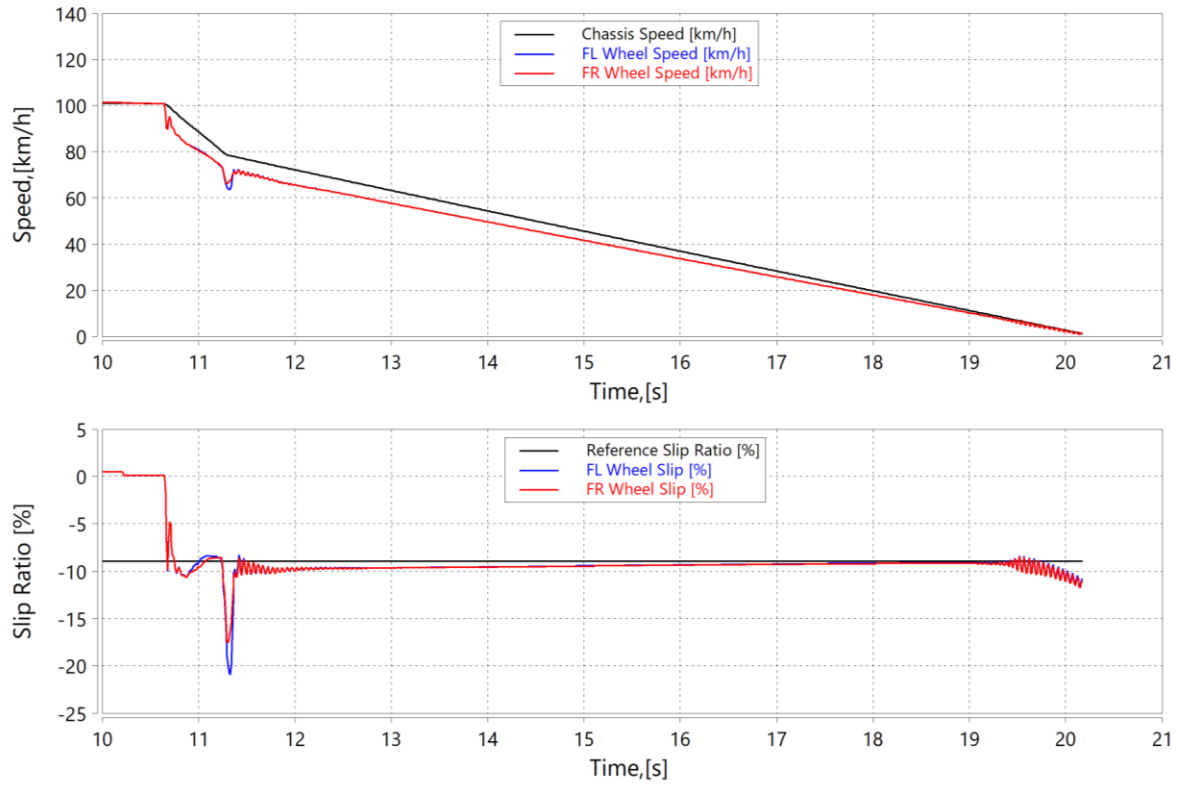

Figure 34. µ-High to µ-Low Sliding Mode Control

Table 9. µ-High to µ-Low KPI comparison

KPI \ ABS controller	Gain PI	SMC
BD [m]	116,0284485	113,1182042
IPV [deg]	1,2434157	1,27721547
IYV [deg]	11,81380534	12,36671698
MD [m/s^2]	2,657332828	2,694319303
MSE [-]	0,101678255	0,082923679
SE [-]	0,093045125	0,063149335

5.2.4. μ - Low to μ - High

μ - Low to μ - High maneuver exhibits similar overshoot as in previous maneuver. Settling time of the SMC controller shown in Figure 37 is again shorter than the settling time of the *Gain Scheduling PI* shown in Figure 36, but this behavior has a drawback of lowering the driving comfort and vehicle stability. *Gain Scheduling PI* has smaller tracking error and a smaller maximum slip error, but the stopping distance of it is still longer than the stopping distance of the SMC. Timestamp of friction coefficient change is shown in Figure 35 and KPIs are given in Table 10.

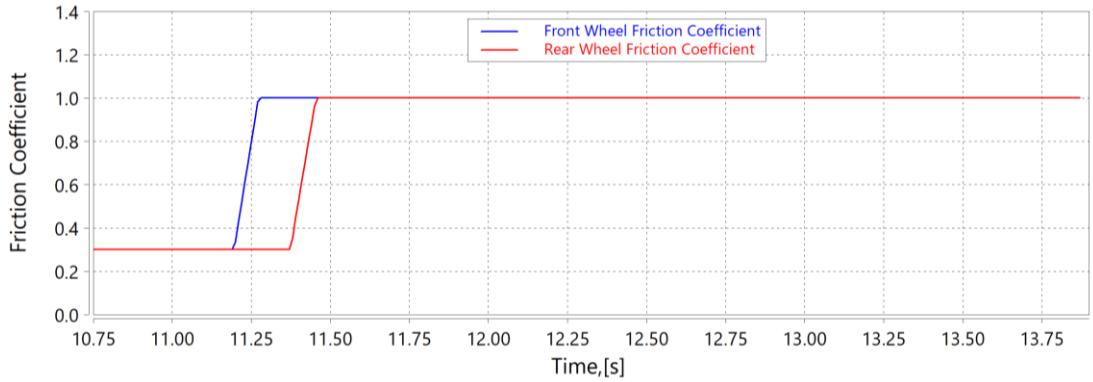

Figure 35. μ-Low to μ-High friction coefficient change

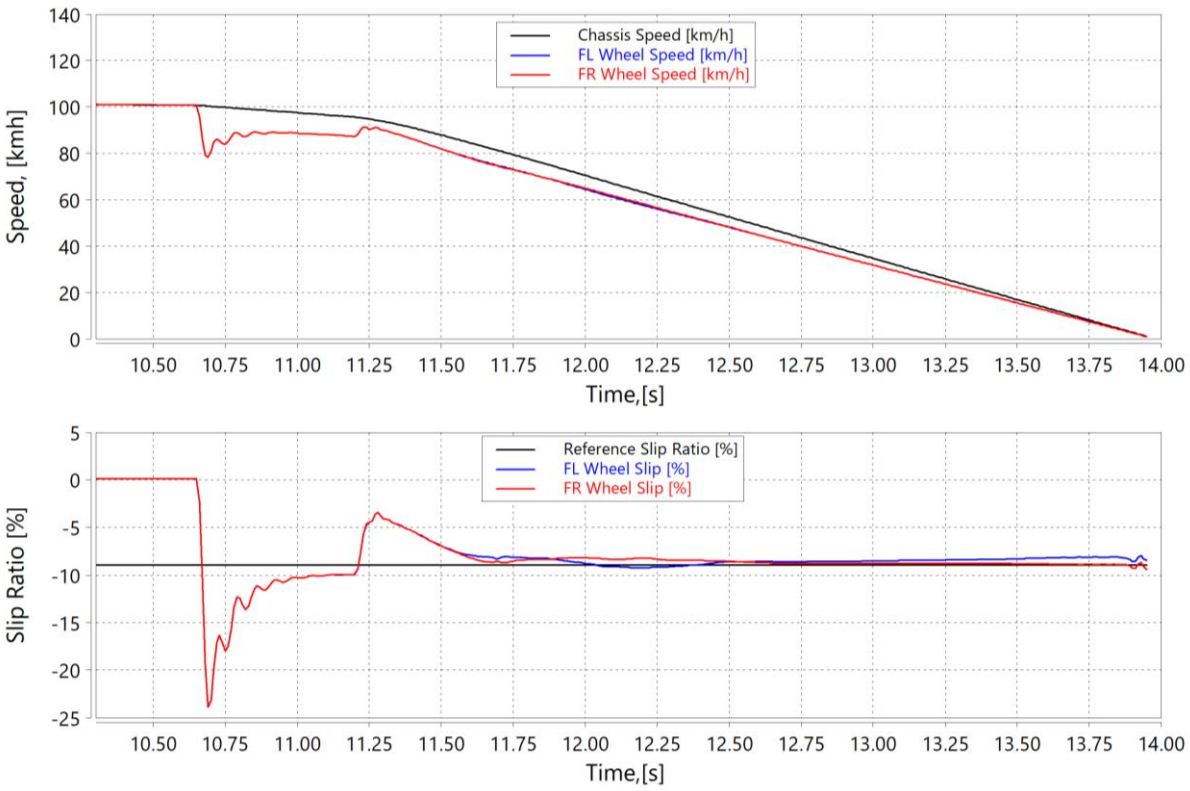

Figure 36. μ-Low to μ-High Gain Scheduling PI

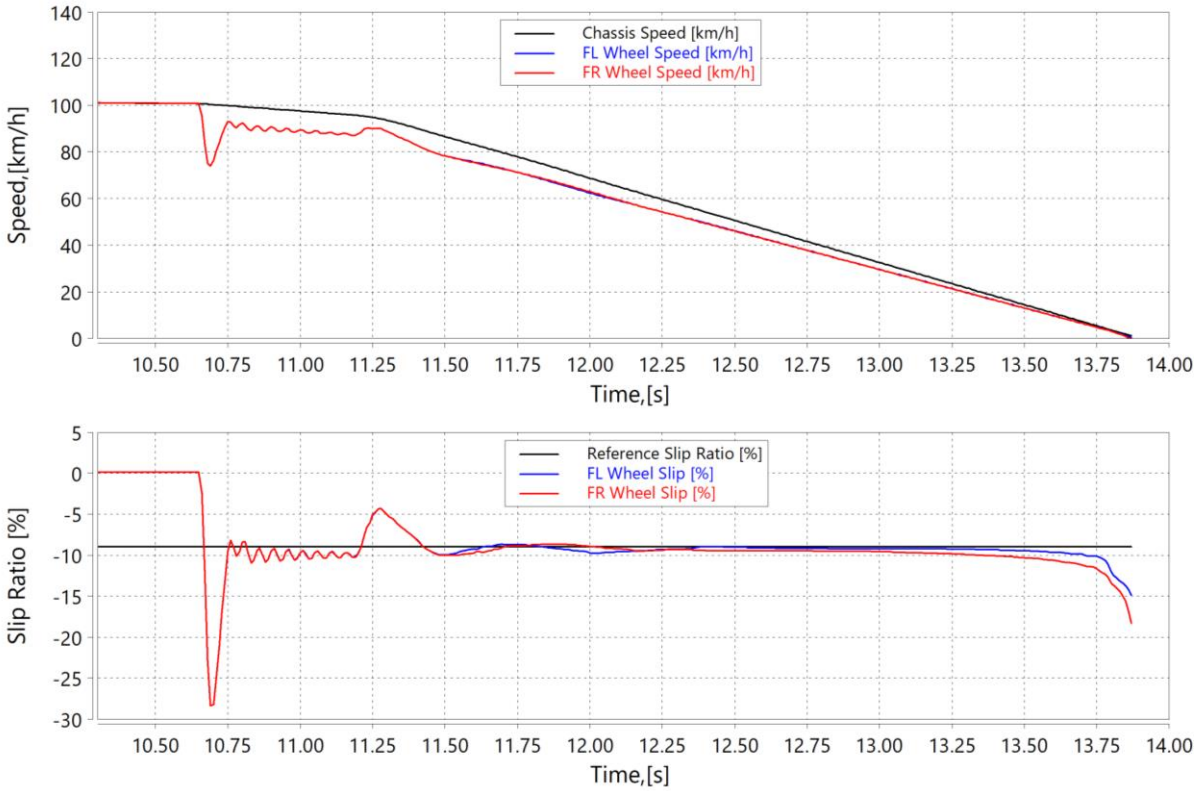

Figure 37. µ-Low to µ-High Sliding Mode Control

Table 10. µ-Low to µ-High KPI comparison

KPI \ ABS controller	Gain PI	SMC
BD [m]	52,51332938	51,13423577
IPV [deg]	2,273522067	2,268978269
IYV [deg]	3,240143284	3,58833799
MD [m/s^2]	9,824424766	10,01845547
MSE [-]	0,135446356	0,176758567
SE [-]	0,10511836	0,153810548

5.2.5. μ - Step

After looking at the two previous maneuvers, the same conclusion can be drawn out from the μ - *Step* maneuver. The SMC controller shown in Figure 40 reacts faster to the transient road changes, but the *Gain Scheduling PI shown* in Figure 39 tracks the setpoint value better in the non-transient conditions. Due to the faster response of the SMC controller, the braking distance is shorter than the braking distance of Gain *Scheduling PI* controller. Timestamp of friction coefficient change is shown in Figure 38 and KPIs are given in Table 11.

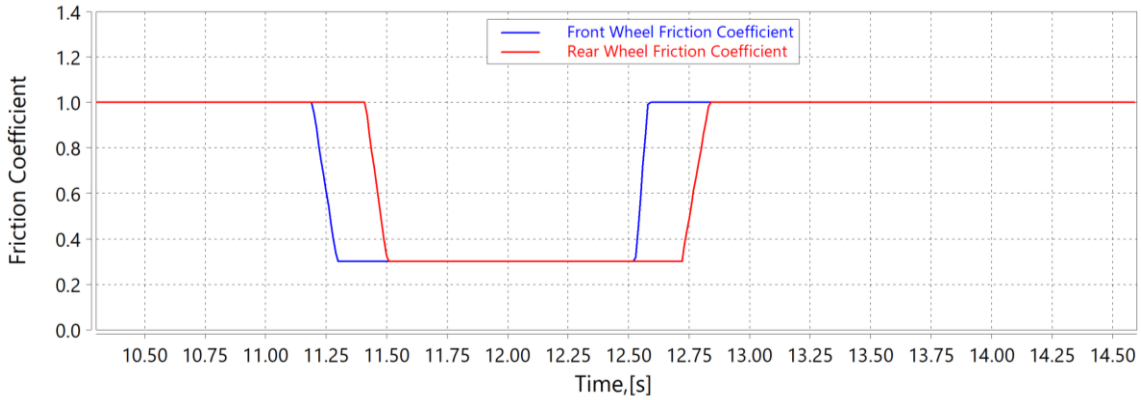

Figure 38. μ-Step friction coefficient change

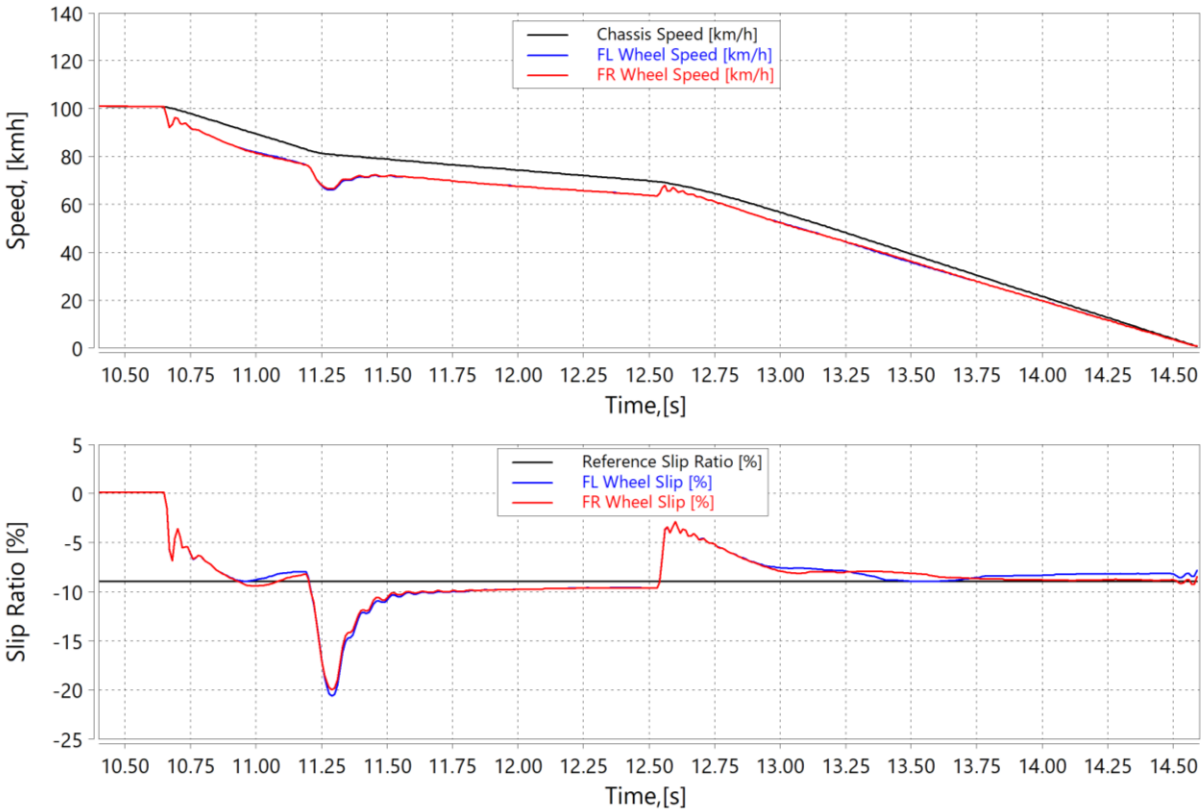

Figure 39. μ-Step Gain Scheduling PI

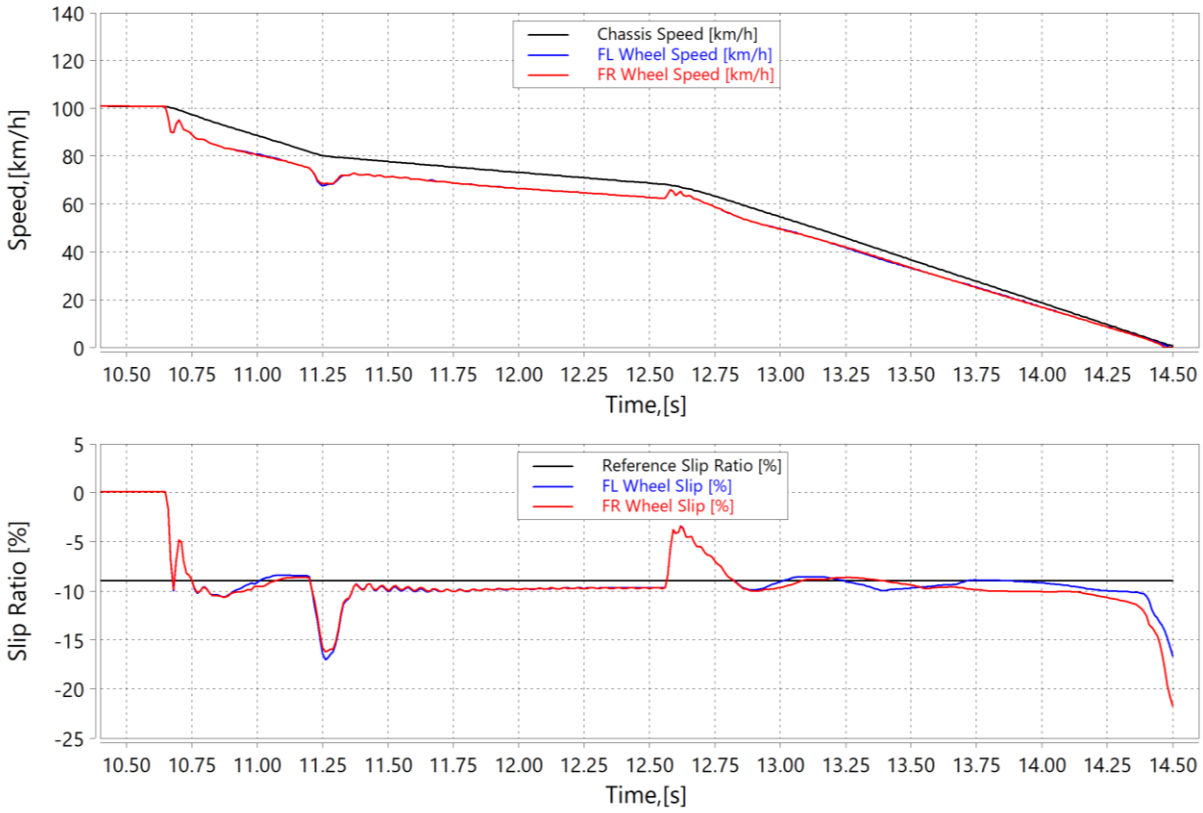

Figure 40. µ-Step Sliding Mode Control

Table 11. µ-Step KPI comparison

KPI \ ABS controller	Gain PI	SMC
BD [m]	63,02380933	61,17880545
IPV [deg]	2,405310368	2,451121279
IYV [deg]	13,33191177	14,4091208
MD [m/s^2]	6,768963318	6,705528689
MSE [-]	0,095127949	0,067188084
SE [-]	0,159342175	0,083452506

5.2.6. μ - Split

μ - Split maneuver exploits the ABS controller robustness, regarding the vehicle stability and the yaw and pitch motions of the vehicle are smaller for the *Gain Scheduling PI* controller. For both controllers the maximum braking torque difference is set to 300 Nm to annulate some of the yaw motion, but the drawback is that the tire that is on the surface with higher friction coefficient, will not use the full traction potential, as it can be seen from Figure 42 and 43. If the limit was set higher, the deceleration would be higher, but more of the yaw motion would be present. *Gain Scheduling PI* controller shows more stability overall and SMC has shorter braking distance. Timestamp of friction coefficient change is shown in Figure 41 and KPIs are given in Table 12. In Figure 44 yaw motion for both controllers is shown.

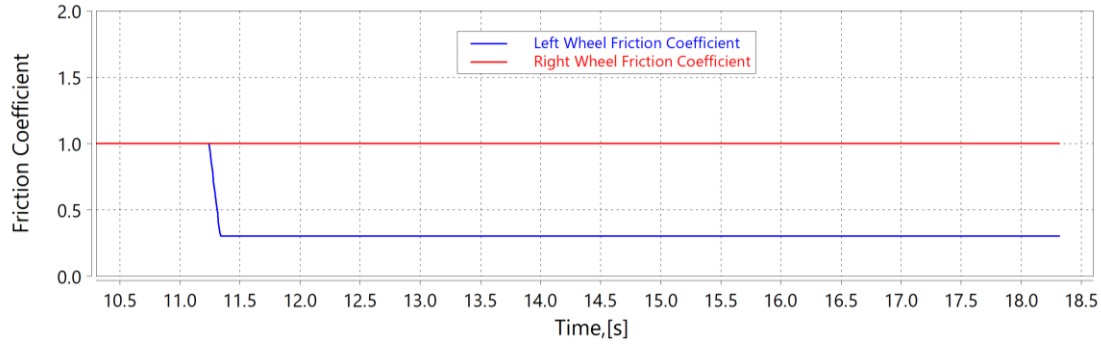

Figure 41. μ-Split friction coefficient change

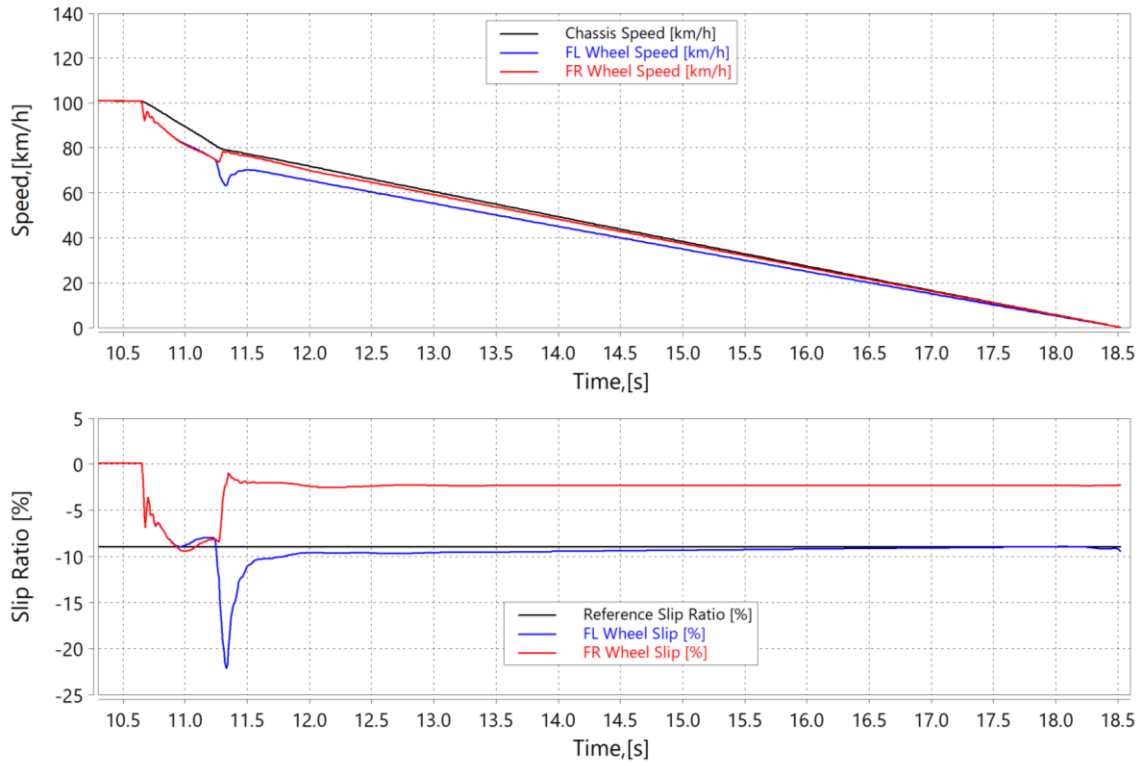

Figure 42. μ-Split Gain Scheduling PI

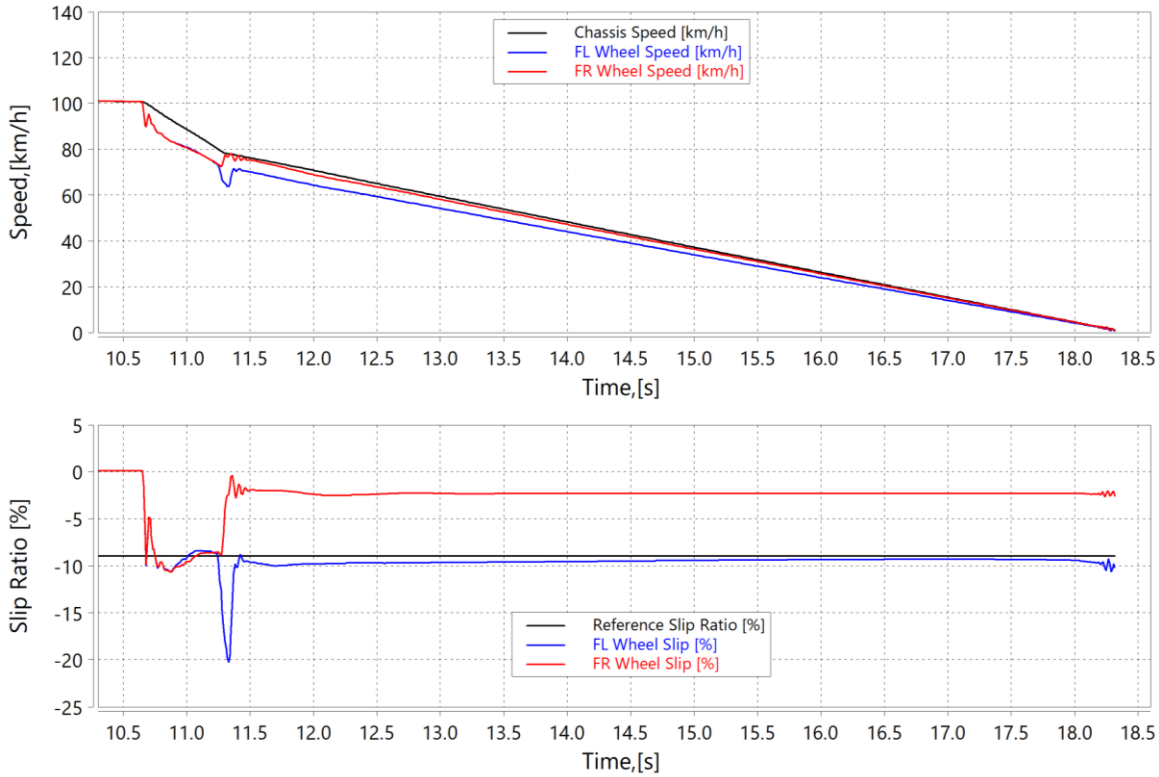

Figure 43. µ-Split Sliding Mode Control

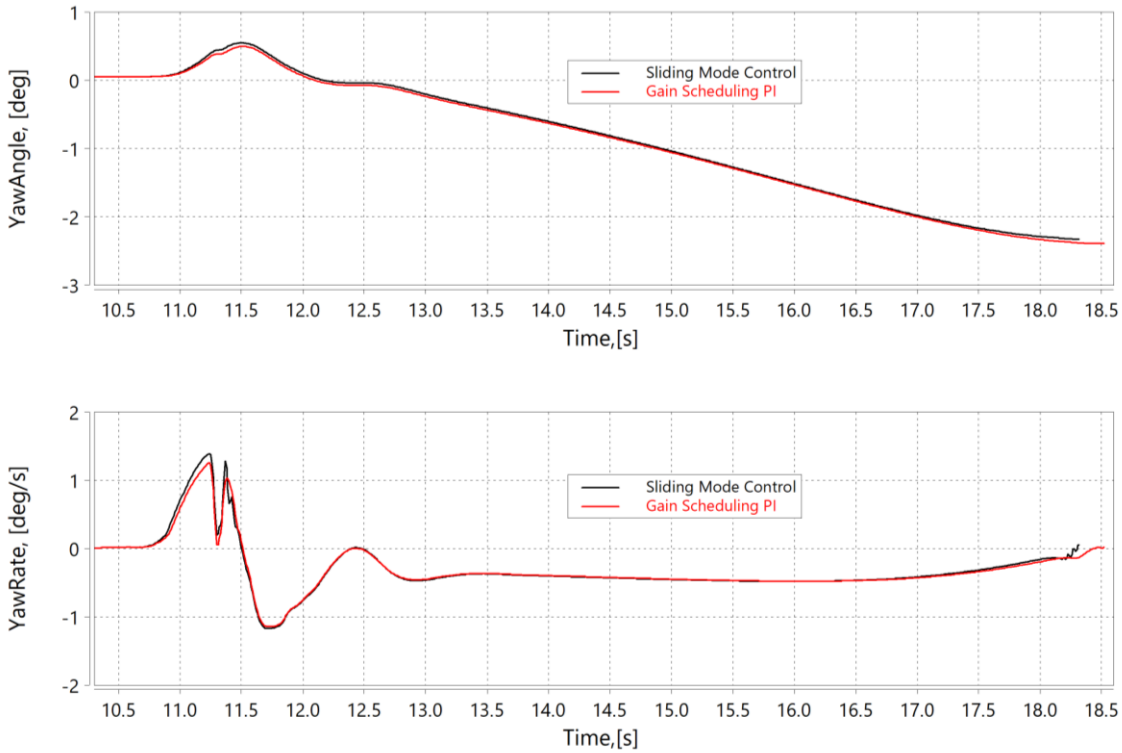

Figure 44. µ-Split yaw motion comparison

Table 12. µ-Split KPI comparison

KPI \ ABS controller	Gain PI	SMC
BD [m]	95,47297985	93,20923
IPV [deg]	3,329752176	3,372176
IYV [deg]	11,2343529	11,72326
MD [m/s^2]	3,33036002	3,2834
MSE [-]	0,0261	0,030437
SE [-]	0,737061433	0,674528

5.3. Relative comparison

To summarize the previous maneuvers and the performance difference between the two proposed controllers, relative comparison charts have been made. Ideal look of the chart would be that the values of KPIs are close to the center, except the mean deceleration. Scale on the chart is ranged from 0 to 100 and these values represent the relative percentage between the both controller KPIs. With that in mind, it is easy to conclude that the SMC controller is a faster and responsive controller when looking at responses to braking command. The drawbacks are occasional overshoots, but sometimes the difference in tire slip overshoots is negligible. In whole, during the non-transient behavior, the *Gain Scheduling PI* tracks the setpoint value of slip ratio better. SMC sometimes due to a lot of uncertainties, has a permanent tracking error which is often barely noticeable, but to extract even more performance out of this controller design, a lot of parameters have to be determined beforehand, so the uncertainty level would be lower. KPIs of mean deceleration and braking distance are almost the same on all maneuvers, which shows that the controllers are successfully tracking the given setpoint, but as already said, when looking at the behavior of a controller from start of the braking to the end differences can be found.

SMC controller in whole would be more suitable in racing applications where the driving comfort isn't the primary goal during braking. Whereas the *Gain Scheduling PI* does not lack noticeably in stopping distance performance, but because of less variations of chassis movements, it is more suitable for everyday use and passenger vehicles where the driving comfort and stability are one of the main talking points when designing a such vehicle. For the configuration with electromechanical brakes on front wheels and electric motors on rear wheels, the *Gain PI Scheduling* controller is chosen due to the all-round performance, and as it is easier

to tune, because of the less uncertainty that enters the tuning and calibration process. Relative comparison charts are provided on following Figures below.

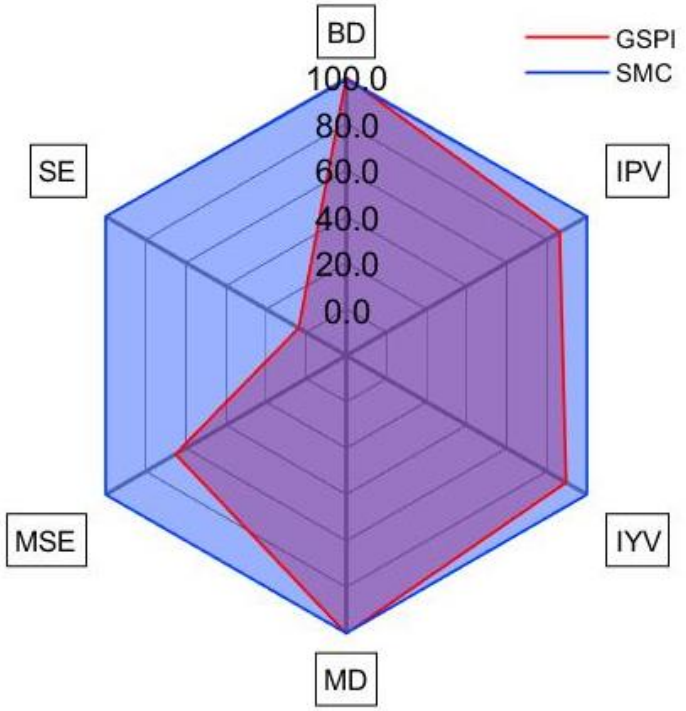

Figure 45. µ-High KPI relative comparison

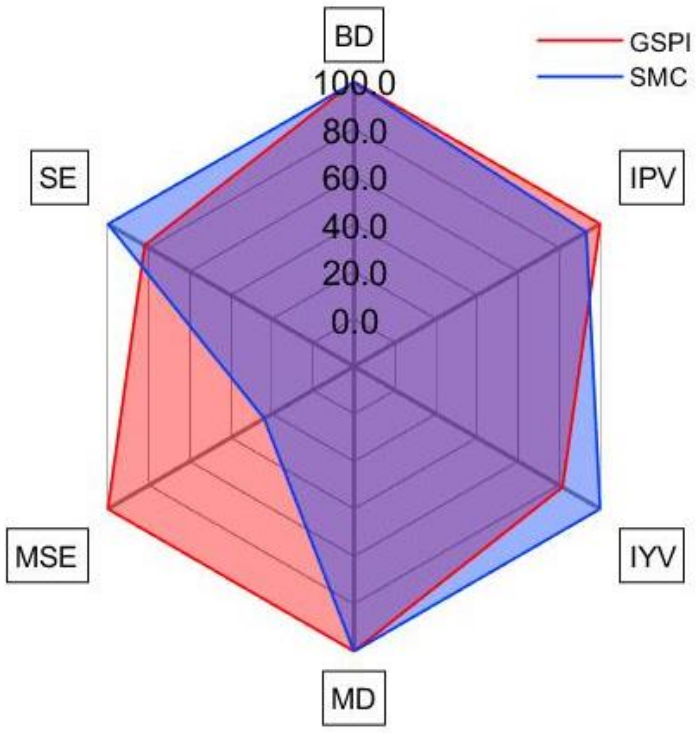

Figure 46. µ-Low KPI relative comparison

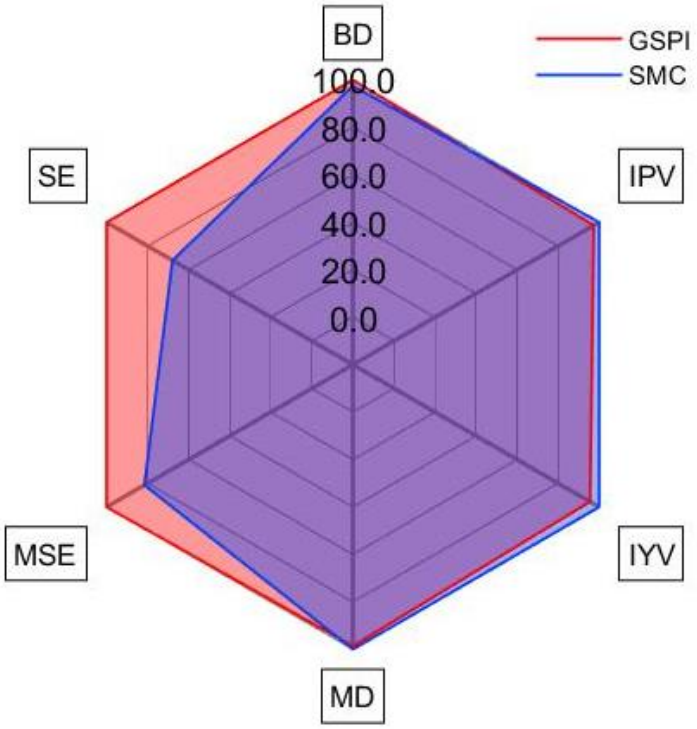

Figure 47. µ-High to µ-Low KPI relative comparison

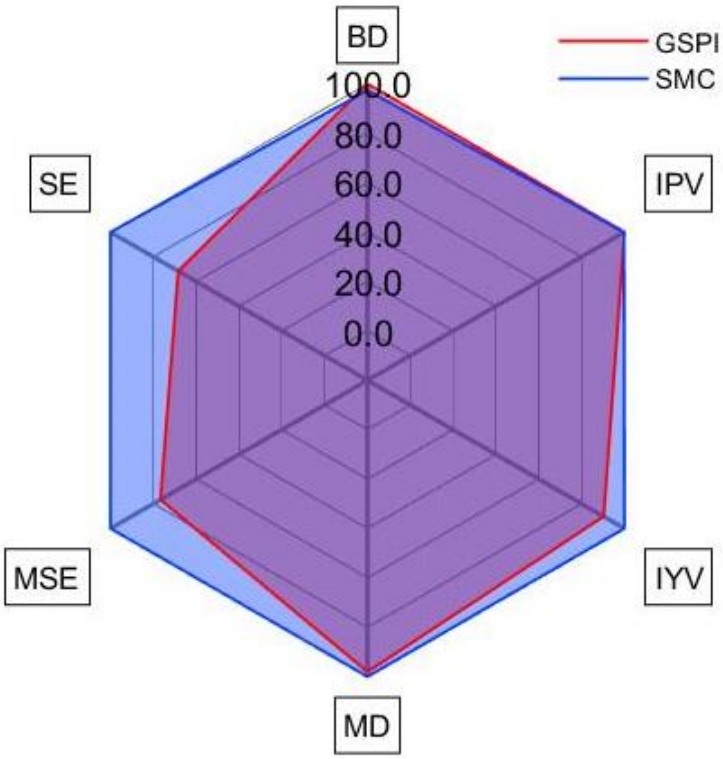

Figure 48. µ-Low to µ-High KPI relative comparison

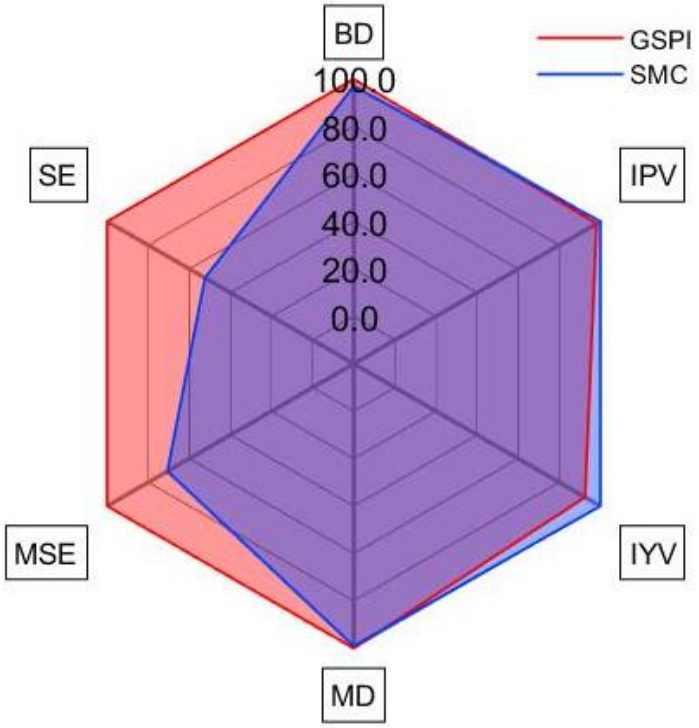

Figure 49. µ-Step KPI relative comparison

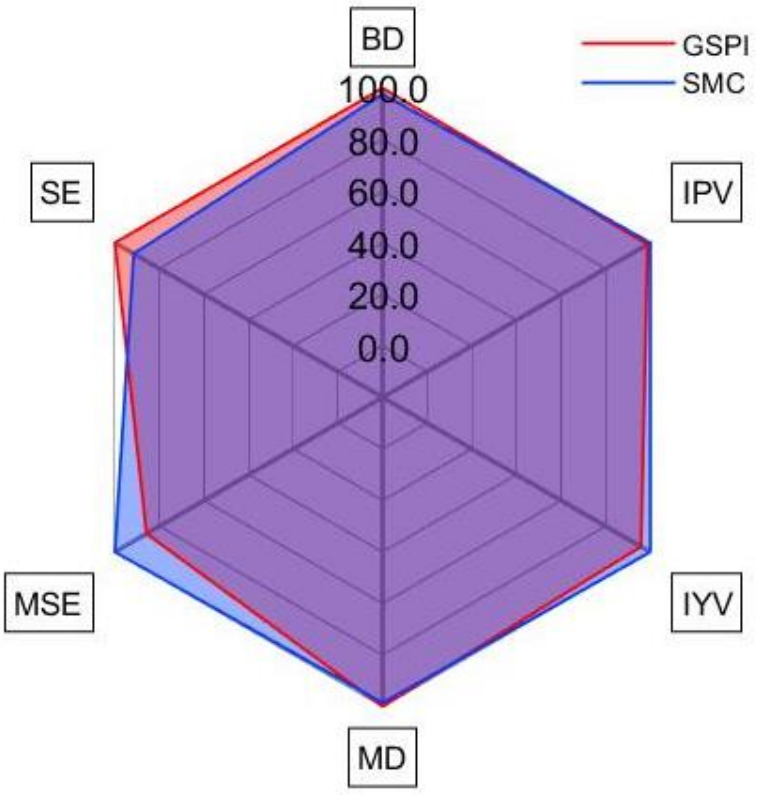

Figure 50. µ-Split KPI relative comparison

5.4. Comparison of proposed ABS controlled EMBs and EMs and conventional ABS

In this chapter, simulation analysis for the second mentioned configuration has been conducted, where the front wheels are braked with electromechanical brakes, and the rear wheels are braked with the help of electric motors. Both electromechanical brakes and electric motor are controlled with the Gain Scheduling PI controller. Measurement data of the real vehicle will be just compared with this configuration, because the first configuration only has the front wheels braked. In scope of this work, real measurements were done on a maneuver μ-High and μ-Low with before mentioned e-Golf 2017, that is equipped with hydraulic brakes, both on front and rear wheels and traction electric motor that is connected to front wheels. Both hydraulic and electric motor brakes were used. In this case μ-Low is slightly differently defined. The starting speed is 70 km/h instead of the before mentioned 60 km/h, and the friction coefficient is equal to $\mu_{low} = 0,2$, so the real and the virtually defined testing maneuver match. Vehicle speed and wheel speeds will be compared, as also the stopping distance of the vehicles, because these are the most tangible key performance indicators in this case.

5.4.1. μ - High

On Figure 51, braking performance of conventional ABS system is shown. The braking starts at the timestamp of 59 s and the targeted wheel slip value is achieved 0,3 s later due to the hydraulic lag. Slip ratio varies from start to finish, between values of 0 and -0,2, and at the very end of braking maneuver the rear wheels almost fully lock up with the slip value of -0,7, as it is seen from the graph. Comparing the timestamps of Figure 51 and 53, it is visible that the vehicle stopped after 2,6 s and the final braking distance is equal to 37,7 m.

On Figure 52, performance of proposed ABS controller is presented. At the start a slight overshoot is exhibited, and the slip value settles after 0,2 s and it remains the same throughout the whole maneuver. From comparison of the timestamps of Figure 52 and 53, is visible that the vehicle stops after 2,2 s and the stopping distance is equal 26,6 m. From previous chapter on μ-High maneuver where just the front EMBs have been braking the stopping distance resulted in around 38,5 m. Even then the difference can be seen, but with all four wheels braked, full traction potential is used.

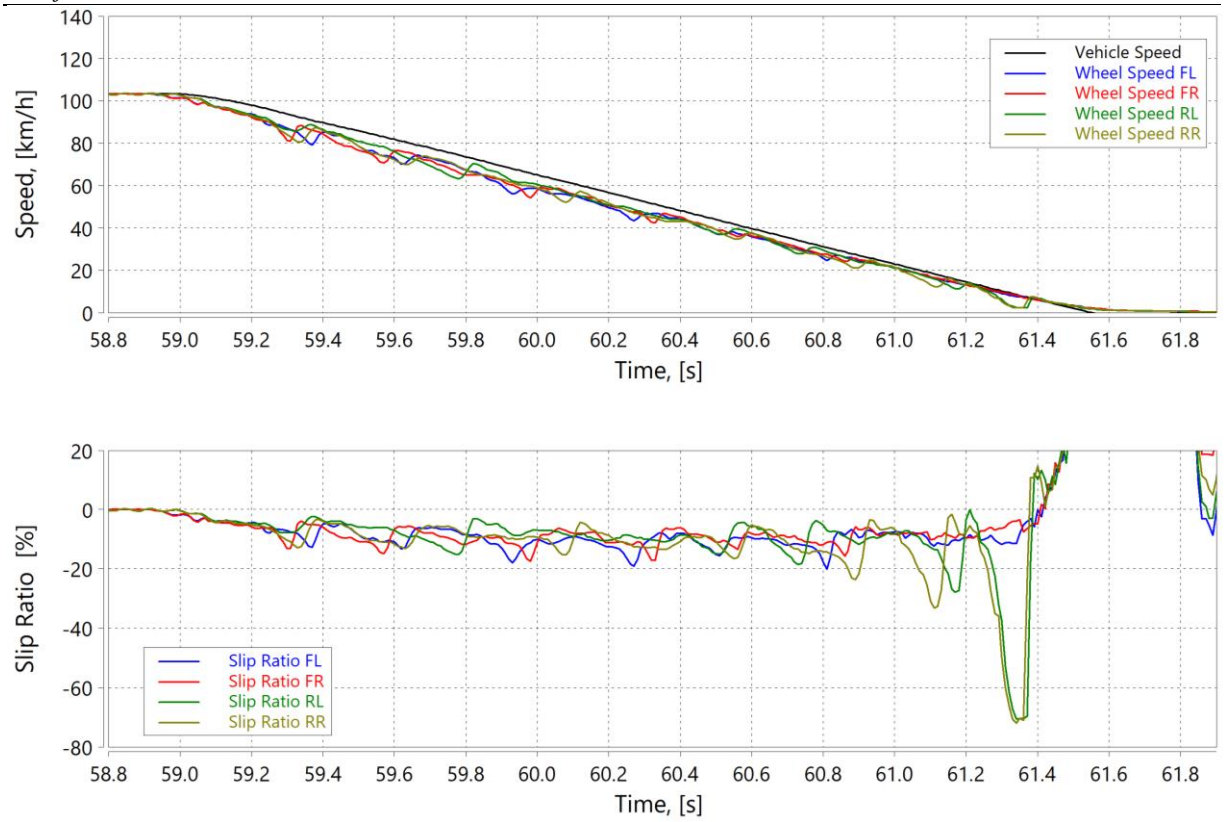

Figure 51. µ-High with conventional ABS system (real measurements)

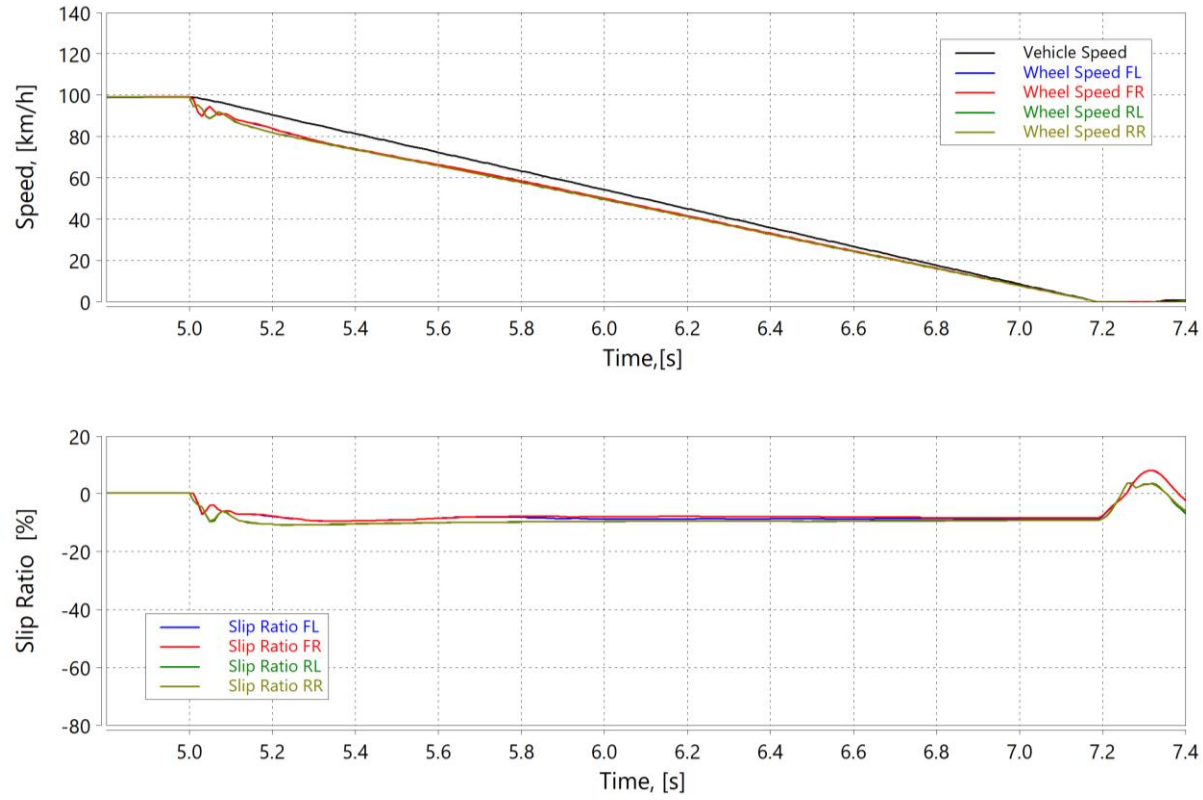

Figure 52. µ-High with Gain Scheduling PI ABS controller

.

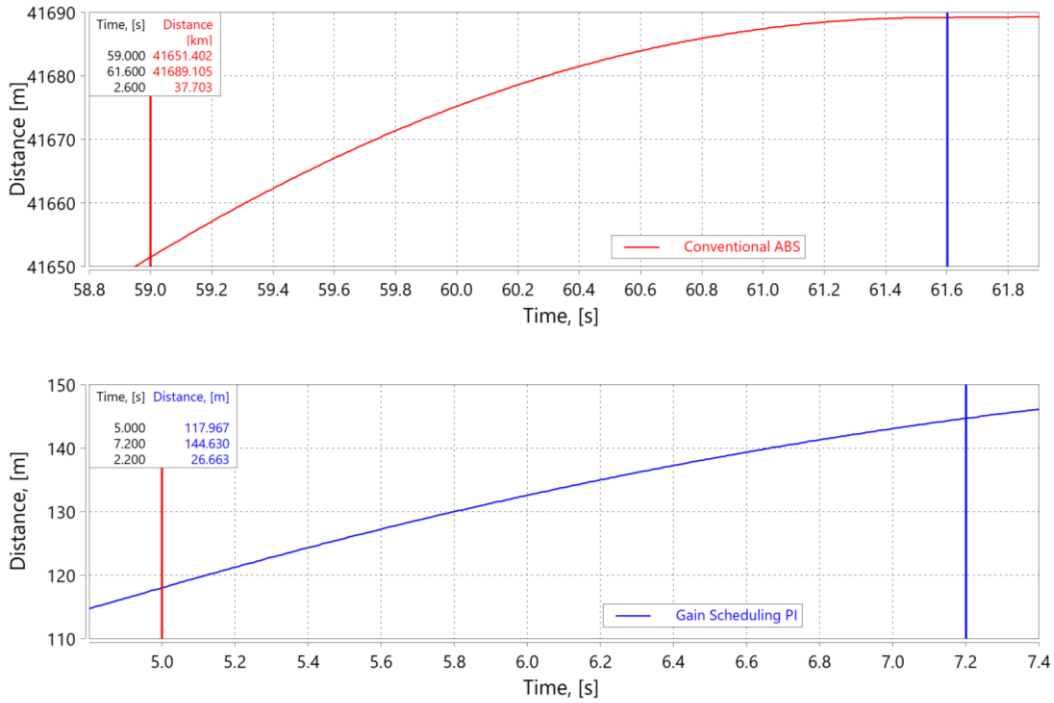

Figure 53. μ-High comparison of stopping distances

The difference between braking distances is great, because of the oscillating wheel speeds. As mentioned in previous chapters, friction coefficient between the tire and road is directly dependent on tire slip ratio. Results on Figure 51 are showing that the slip ratios are overshooting optimal value often and they are often equal to zero, and therefore the maximum traction potential isn't used. Whereas at Figure 52 the optimal slip value is tracked, without the appearance of large oscillations, therefore the full traction potential is used.

5.4.2. μ - Low

On Figure 54, braking performance of conventional ABS system is shown. The braking starts at the timestamp of 14,7 s. From the start of the braking to the very end of the braking maneuver, the oscillations of wheels speeds are rising, to the point where the slip value is equal to -0,7. Due to the oscillations the full traction potential can't be achieved and the braking distance of a vehicle equipped with conventional ABS systems is equal to 195,5 m as seen from Figure 56.

On Figure 55, performance of the proposed ABS controller is seen. Front electromechanical brakes cause a slip of -0,3 at the start of the braking, but the value settles after 0,2 s. Electric motors have a faster response and they have a smaller overshoot value of -0,18 and the settling time is equal to 0,1 s.

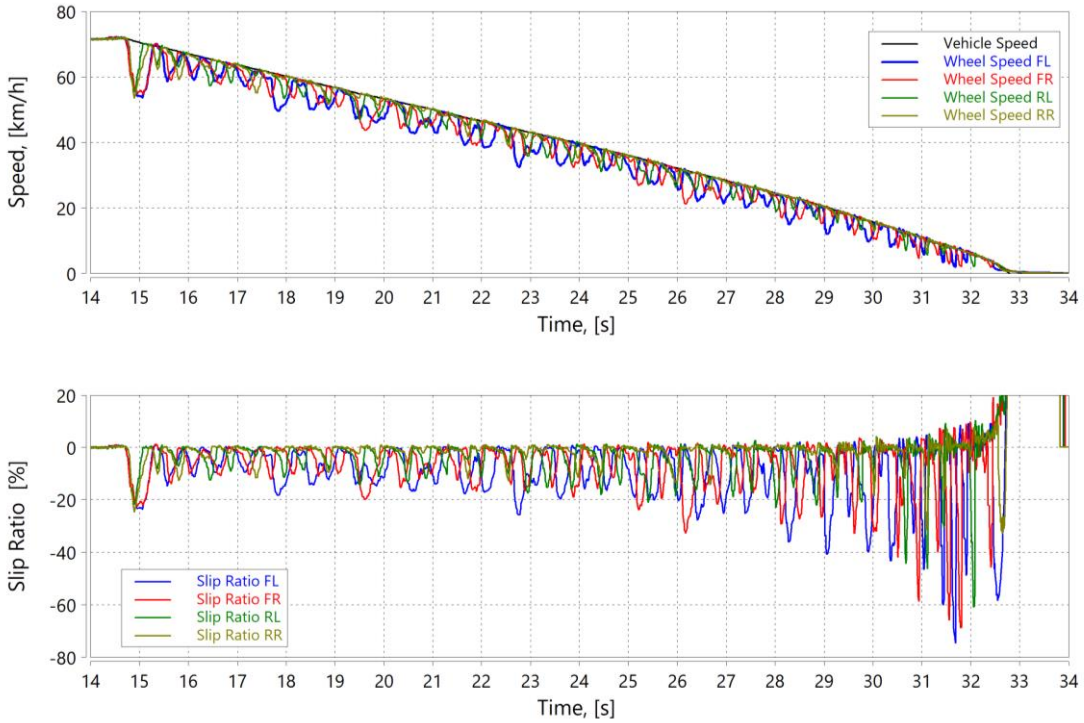

Figure 54. μ-Low with conventional ABS system (real measurements)

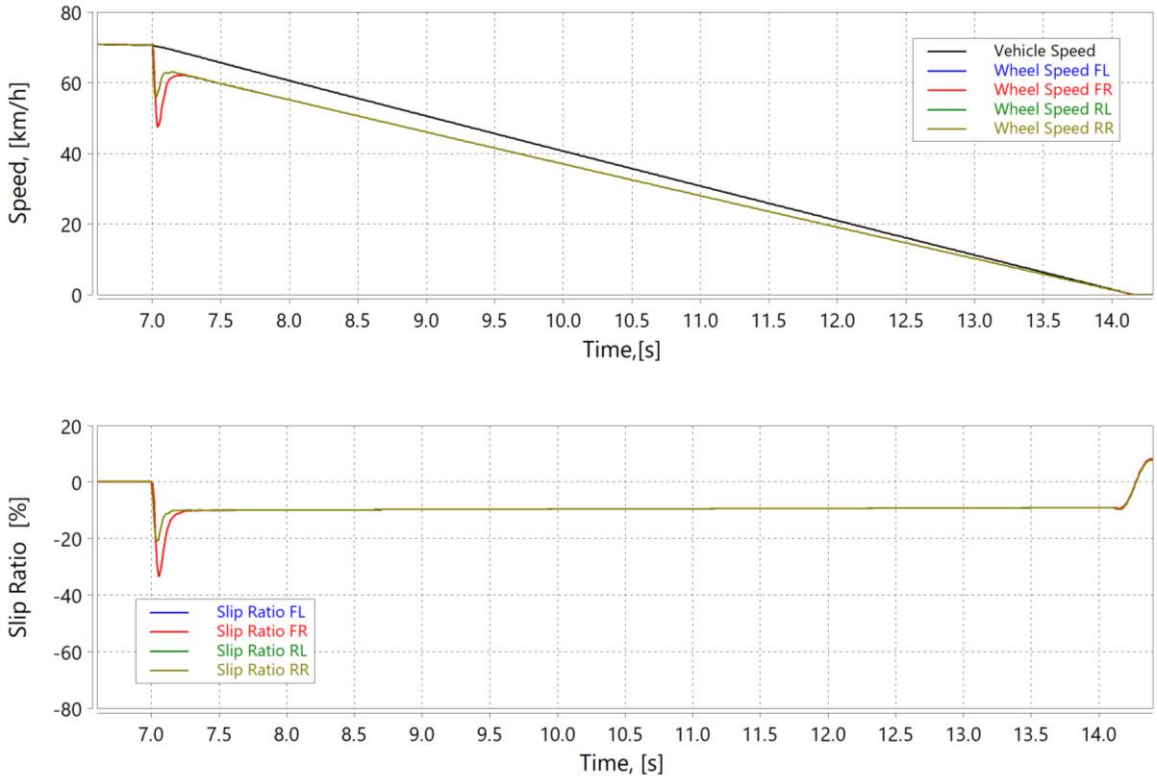

Figure 55. μ-Low with Gain Scheduling PI ABS controller

After settling the setpoint slip value is followed closely without oscillations and the maximum traction potential is used. Because of the mentioned behavior, braking distance for the vehicle equipped with proposed ABS controller has a stopping distance of 69,7 m as shown in Figure 56, which is a great improvement comparing to the conventional ABS system.

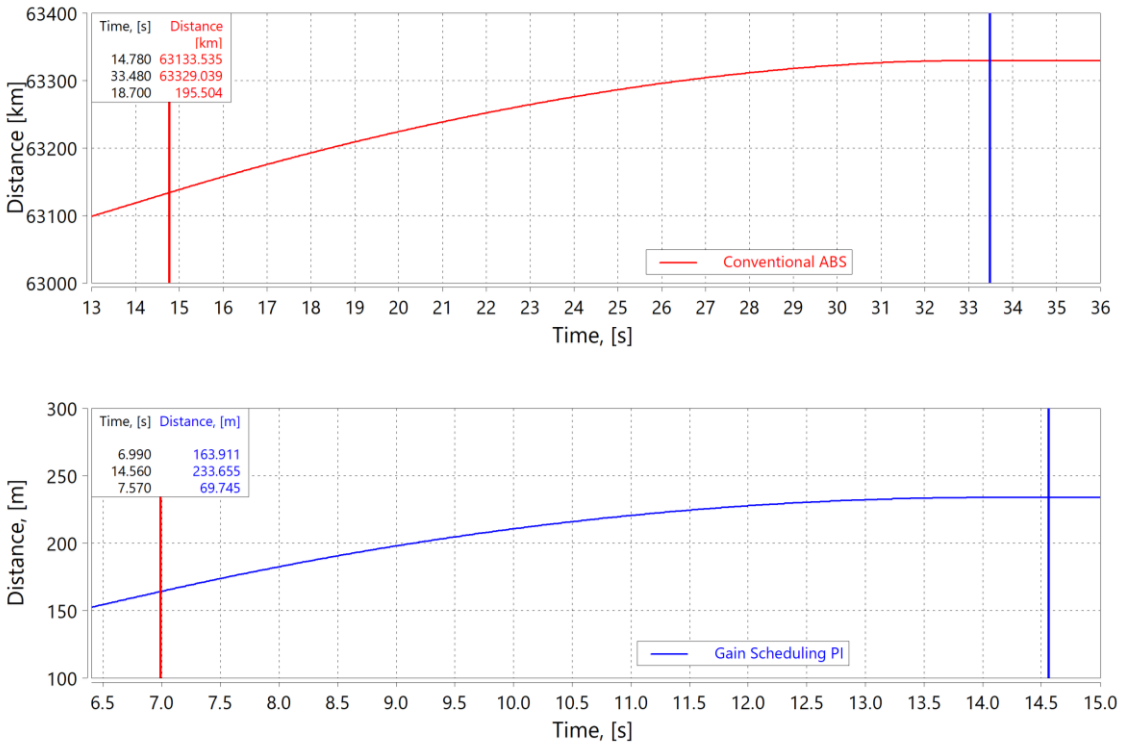

Figure 56. μ-Low comparison of stopping distances

6. CONCLUSION

The main goal of this thesis was to analyze the feasibility of ABS controlled *brake-by-wire* systems through simulation environment, and how the overall performance would compare against conventional hydraulic ABS systems. In order to ensure that the calibrated ABS controllers are robust, simple electromechanical and electric motor brake actuator models have been built up. Dynamics of the mentioned systems acts as a torque response delay and the sample rate of the measured signals has been downsampled from 2000 Hz to 100 Hz, to mimic the calculation time of real automotive system hardware. Proposed designs of ABS controllers have been built up in MATLAB/Simulink® environment together with actuator dynamics. After that, the above-mentioned controllers have been coupled with AVL VSM™ software in a co-simulation environment. Vehicle model and tire parameters have been defined in AVL VSM™ that there is as little as possible difference between the simulation model and real vehicle. After the co-simulation environment has been defined and built up, 6 typical braking maneuvers have been defined in AVL VSM™ (*μ - High, μ - Low, μ - High to μ - Low, μ - Low to μ - High, μ - Step and μ - Split*). Mentioned maneuvers have been simulated with the *Gain Scheduling PI* and *Sliding Mode Controller.* Before the simulation analysis key performance indicators have been defined as an evaluating system of the before-mentioned controllers. Simulation analysis was conducted on a configuration with electromechanical brakes mounted on front wheels and the results and relative comparison between the two controllers have been given.

Results have been examined and compared and *Sliding Mode Controller* showed as a faster acting controller with better performance in terms of stopping distance, but with drawback with lower driving comfort and stability. *Gain Scheduling PI* controller has longer stopping distances than the *Sliding Mode Controller*, but as the difference is negligible, due to more applicability to passenger vehicles *Gain Scheduling PI* controller has been chosen to compare with the conventional ABS systems. Again, simulation analysis was conducted on second brake layout configuration where electromechanical brakes are mounted on to the front wheels and electric motors on the rear wheels. On a *μ - High* maneuver, *Gain Scheduling PI* controller had a braking distance of 26,6 m, whereas the conventional ABS system had a braking distance of 37,7 m. On a *μ - Low* maneuver, *Gain Scheduling PI* controller had a braking distance of 69,7 m, whereas the conventional ABS system had a braking distance of 195,5 m. In both cases the improvement is easily visible, especially on the low friction surfaces.

To summarize, two brake-by-wire ABS controllers were implemented and tested successfully for both brake layout configurations. *Gain Scheduling PI* controller showed less oscillations during braking, and less vehicle yaw and pitch motions which is suitable for passenger vehicles. Finally, the mentioned controller was compared with conventional ABS system, where great improvements have been noticed, in terms of wheels speed oscillations and vehicle braking distances, and therefore the feasibility of *brake-by-wire* systems and its controller has been proved.

The proposed improvements and further work are as follows:

- investigation of friction coefficient estimation as a scheduling variable or tuning parameter for road transient conditions
- building up a vehicle speed estimator that is going to be used when all four wheels are braked
- implementation of detailed mathematical model of electromechanical brakes and electric motors
- validation of proposed controllers in demonstrator vehicle

LITERATURE

[1] *Conventional ABS system.* https://www.semanticscholar.org/paper/Modeling%2C-design-and-control-of-an-individual-wheel-Duifhuizen-Hobo/09ca859d81b6576260475ac53038fed9bc397aae , 31.03.2020.

[2] *Hysteresis loop.* https://appmeas.co.uk/resources/pressure-measurement-notes/what-are-hysteresis-errors/ , 31.03.2020.

[3] *Vienna Engineering Electromechanical Brake*, 2018.

[4] Park G. Choi S. B. *Clamping force control based on dynamic model estimation for electromechanical brakes*, 2017.

[5] *Mathematical and experimental models.* https://x-engineer.org/graduate-engineering/modeling-simulation/systems-modeling/methods-of-mathematical-modeling/ , 01.04.2020.

[6] Mellodge P. *A Practical Approach to Dynamical Systems for Engineers*, 2016

[7] *Piecewise linear approximation*, https://optimization.mccormick.northwestern.edu/index.php/Piecewise_linear_approximation, 20.04.2020.

[8] Li W. *ABS Control on Modern Vehicle Equipped with Regenerative Braking*, 2010.

[9] Petersen I. *Wheel Slip Control in ABS Brakes using Gain Scheduled Optimal Control with Constraints,* 2003.

[10] Zhang R., *Study on Self-Tuning Tyre Friction Control for Developing Main- Servo Loop Integrated Chassis Control System*, 2017

[11] Pacejka H. B. *Tyre and Vehicle Dynamics*. Butterworth-Heinemann, 2006.

[12] Solyom S. Rantzer A. Ludemann J. *Synthesis of a Model-Based Tire Slip Controller*. Vehicle System Dynamics, 2004.

[13] J. J. E. Slotine, W. Li *Applied Nonlinear Control,* Prentice Hall, 1991.

[14] Yoon P. Kang H. Hwang I. *Braking Status Monitoring for Brake-By-Wire Systems*. X-By-Wire Automotive Systems, 2004.

[15] Drakunov S. et al. *ABS Control Using Optimum Search via Sliding Modes.* IEEE Transactions on Control Systems Technology, 1995.

[16] Wang Y. Bevly D. M. *Longitudinal tire force estimation with unknown input observer*, 2012.

[17] *e-Golf 2017*. https://pod-point.com/guides/vehicles/volkswagen/2017/e-golf , 20.04.2020

[18] Pretagostini F. *Anti-lock braking control design using a Nonlinear Model Predictive approach and wheel information*, 2018.